METEOROLOGICAL CHARACTERISATION OF THE FEBUKO HILL CAP CLOUD EXPERIMENTS

PART II: TRACER EXPERIMENTS AND FLOW CHARACTERISATION WITH NESTED NON-HYDROSTATIC ATMOSPHERIC MODELS

B. Heinold[1#], A. Tilgner[1], W. Jaeschke[2], W. Haunold[2], O. Knoth[1], R. Wolke[1]
and H. Herrmann[1]

[1]Leibniz-Institut für Troposphärenforschung, Permoserstr. 15, 04318 Leipzig, Germany
[2]Johann-Wolfgang-Goethe Universität Frankfurt, Zentrum für Umweltforschung, Georg-Voigt-Str. 14, 60325 Frankfurt a.M., Germany

ELECTRONIC SUPPLEMENTARY MATERIAL (ESM)

Key word index: flow over complex terrain, FEBUKO, flow parameters, flow modelling, tracer studies.

 # Corresponding author: e-mail: heinold@tropos.de, tel.: +49-341-2352822, fax: +49-341-2352139

Supplemental material for the SF_6 tracer experiments (section 2.4)

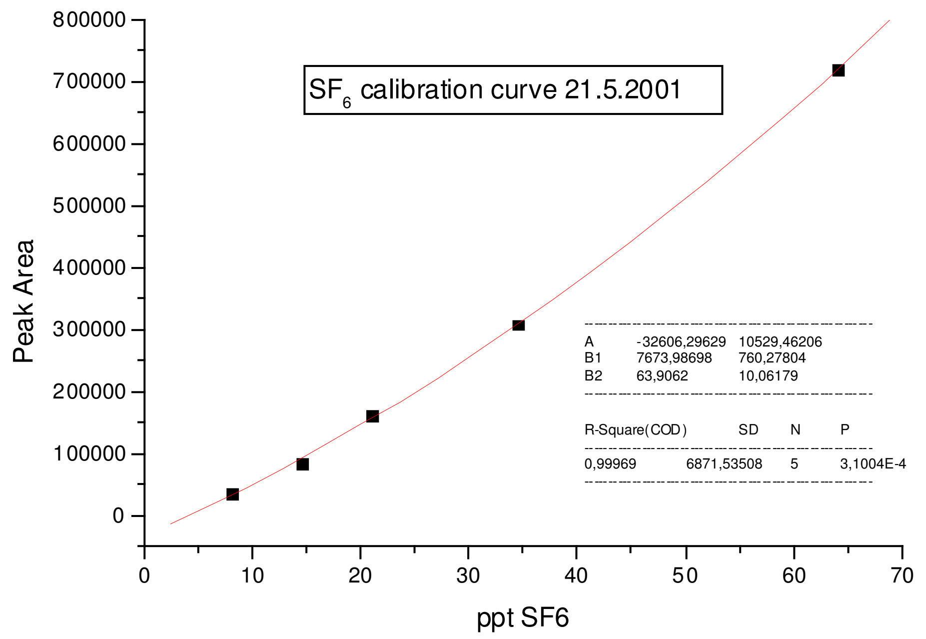

Fig. I. Calibration curve from 21-05-2001.

Detailed description of LM results for 2, 6 – 8, 26 and 26/27 October 2001 and 16/17 October 2002 (section 3.2)

2 October 2001

On 2 October 2001 the wind blew constantly from southwest with wind speeds up to 12 m s^{-1}. The stable flow conditions are also reflected in the LM results. Figure 3a presents the horizontal surface winds for the innermost domain for 2 October 2001 at 12:00 UTC. As to be seen the flow structure is very homogeneous with wind speeds of 10 – 20 kn (~ 5 – 11 m s^{-1}). Due to the strong wind the orography hardly has an effect on the flow. Only downstream from the Rhön channelling of flow occurs along the Werra valley and a little deceleration is evident from the wind speed decreasing from 15 kn (~ 8 m s^{-1}) to 10 kn (~ 5 m s^{-1}) just before the ridge. The experimental site itself is located in a zone of straight southwesterly flow. However, the predominantly homogeneous flow pattern and the high wind velocities imply that the air passes over the mountain range. In consequence of the overflow the LM predicts lee waves evident from the up and down of isentropes in Figure 4a. This is in agreement with rawinsonde data, which show a weak inversion in about 1800 m asl and a distinct increase in wind speed with height. Both the stable atmospheric stratification with weakening above the inversion and the wind shear provide a basis for lee wave formation. Also satellite pictures in Tilgner et al. (2005) prove the model-predicted lee waves.

6 – 8 October 2001

The flow conditions from 6 October 2001 to the early morning hours on 8 October 2001 were characterised by low wind speeds of about 5 kn (~ 2.6 m s^{-1}) and unstable winds from south on windward side. On the ridge and downwind the modelled surface wind turns to southwest. The different wind directions indicate that the air passes around rather than over the mountain range. But on 8 October 2001 the blocking weakens because the wind speed slightly increases and the wind direction changes from south to southwest on the lee side during daytime (Figure 3b).

26 October 2001

On 26 October 2001 the meteorological conditions were generally very stable including a stable atmospheric stratification. But the stable conditions seem to be unfavourable with respect to the overflow of the Thüringer Wald. As can be seen in Figure 3c the local flow at 09:00 UTC is directed from south on the windward side with channelling of airflow in the Werra valley. Northwest and southeast of the mountain range the air tends to flow around the ridge. The vertical cross section of isentropes (Figure 4b) shows air falling down from higher altitudes to the downwind site in a hydraulic jump. This refers to overturned gravity waves and results in different air masses at the experimental sites.

26/27 October 2001

The event on 26/27 October 2001 provides more appropriate flow conditions. This episode was characterised by a front passage which ended just around 06:00 UTC on 27 October 2001 and divided the flow situation into two periods. At the beginning the modelled flow was southeast with wind speeds of about 5 kn (~ 2.6 m s^{-1}). Channelling occurs in the upper Werra valley and the upwind flow runs parallel to the Thüringer Wald. Northwest and southeast of the mountain range the flow is deflected around. Evidently there is a strong blocking effect due to low wind speeds. Because of differences of wind speed and direction between the valleys and the ridge the flow is assumed to be uncoupled between the different sites. After the end of frontal processes the wind direction gradually changes, the wind speed increases and thus the flow conditions are expected to become appropriate. From 09:00 UTC the wind pattern is characterised by predominantly southwesterly flow (Figure 3d). Only downwind from the Rhön the orientation of wind barbs signalises channelling again. On the most upper part of the Werra valley very low wind velocities and even calm occur. But especially the central part of Thüringer Wald including the experimental site is located in a wide zone of southwesterly flow. The wind speeds are 5 – 10 kn (~ 2.6 – 5 m s^{-1}) at the upwind side and 10 – 15 kn (~ 5 – 8 m s^{-1}) on the ridge and downwind.

Therefore, the air passes over the mid mountain range only with little blocking effects in the second period of this event. On 27 October 2001 the LM simulates several wave regimes. Up to an altitude of 2000 – 2500 m asl lee waves with small amplitude and in atmospheric layers above vertically propagating gravity waves which reaches the upper boundary of model domain are formed (Figure 4c). These waves have only a single wave crest over the mountain ridge and a single wave minimum on the lee side. The wave valley leads to a significant intensification of wind indicated by closer streamlines on the upwind slope.

16 – 17 October 2001

A comparable flow situation like on 2 October 2001 also exists from 16 to 17 October 2002. High wind speeds up to 20 kn (~ 11 m s^{-1}) as well as a less complex flow pattern with only minor channelling in the Werra valley and negligible upwind deceleration meet the required flow conditions. In this case the air flow crossing the Thüringer Wald does not include any noticeable wave regime. Obviously the necessary atmospheric conditions for the formation of gravity waves are not satisfied.

Results of LM simulations for some other days/events (section 3.2)

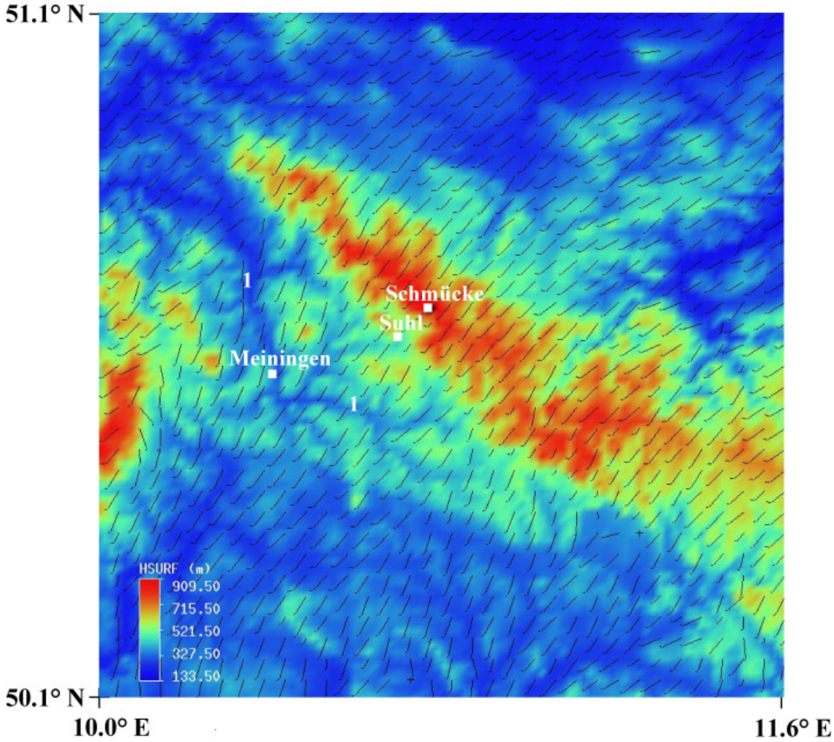

Fig. II. Horizontal cross section of the topography and the surface wind plotted at every third grid point for the innermost LM domain for 06-10-2001 at 12:00 UTC. The wind barbs are in knots. 1: Werra valley.

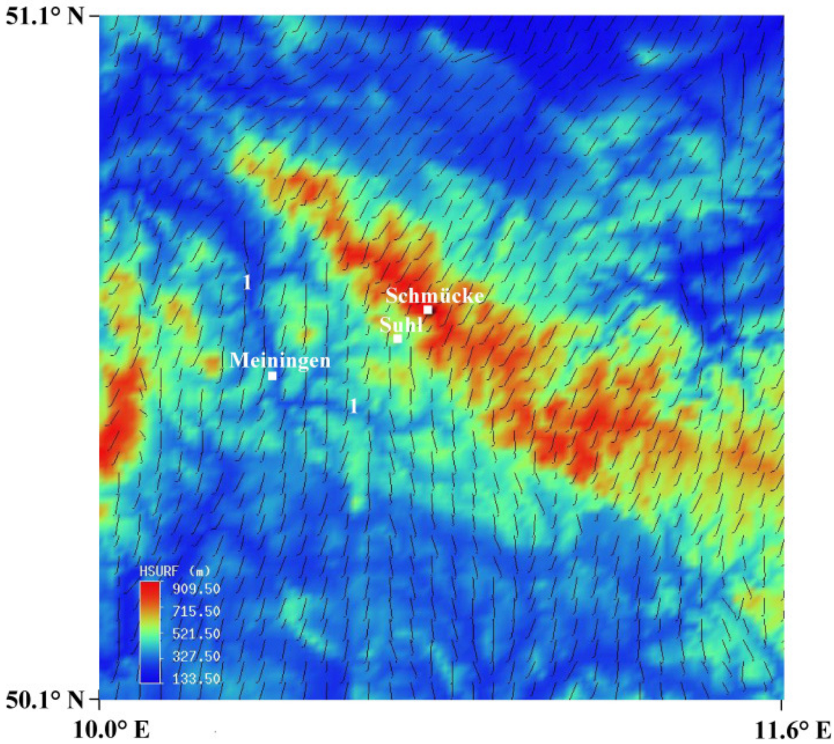

Fig. III. Horizontal cross section of the topography and the surface wind plotted at every third grid point for the innermost LM domain for 07-10-2001 at 14:00 UTC. The wind barbs are in knots. 1: Werra valley.

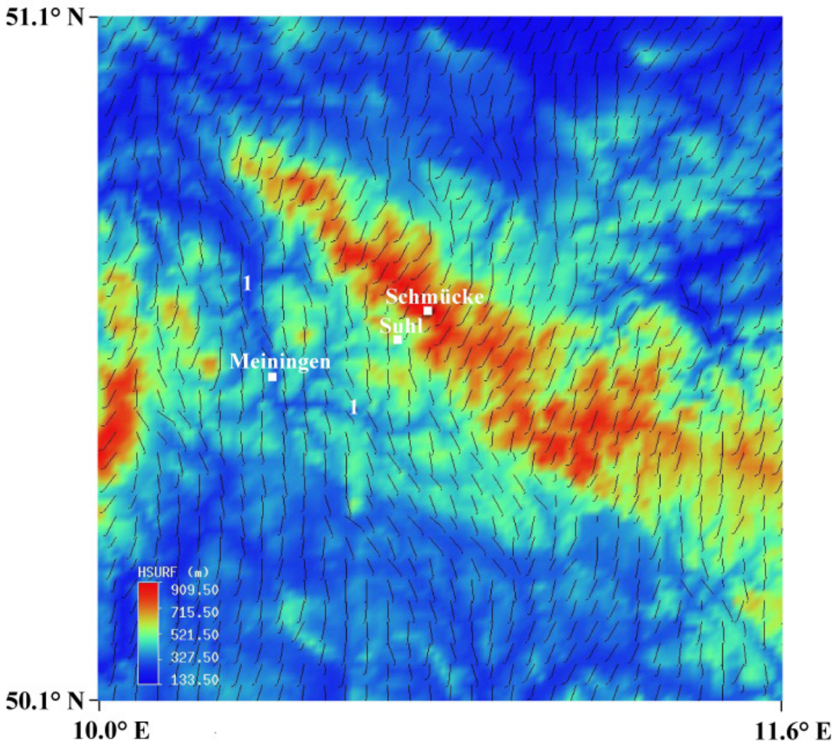

Fig. IV. Horizontal cross section of the topography and the surface wind plotted at every third grid point for the innermost LM domain for 07-10-2001 at 18:00 UTC. The wind barbs are in knots. 1: Werra valley.

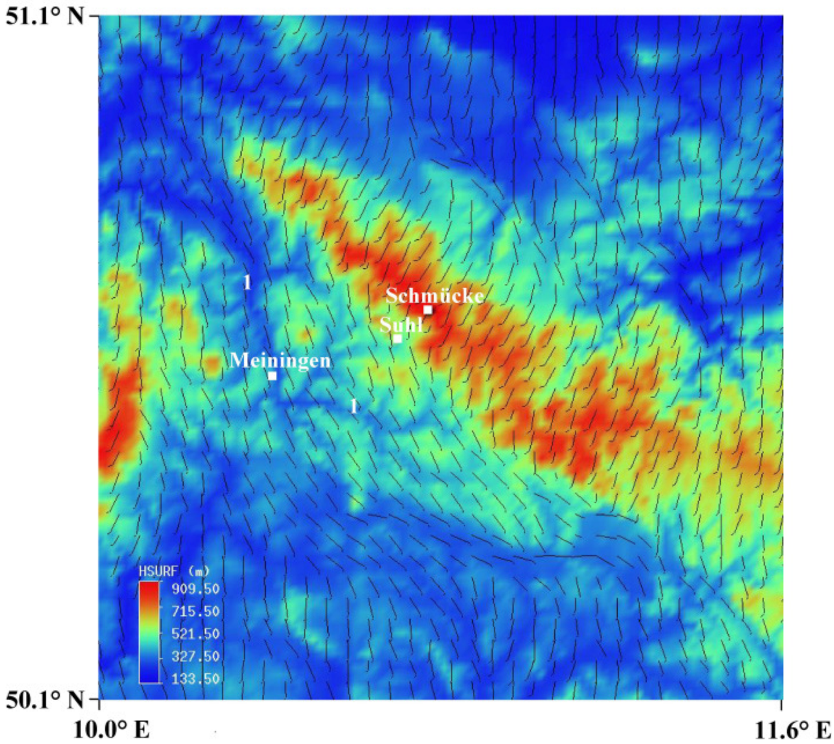

Fig. V. Horizontal cross section of the topography and the surface wind plotted at every third grid point for the innermost LM domain for 08-10-2001 at 00:00 UTC. The wind barbs are in knots. 1: Werra valley.

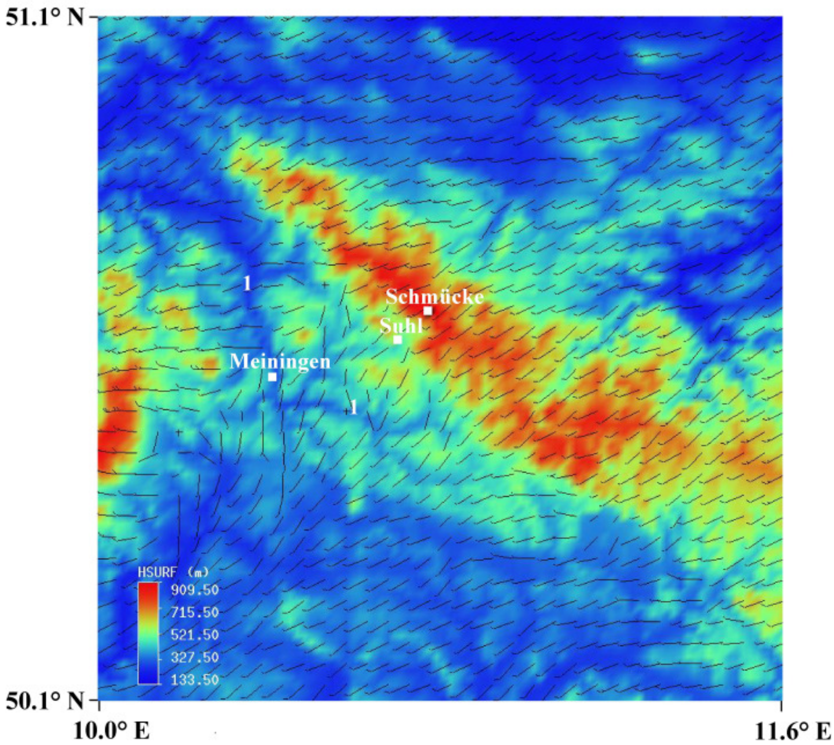

Fig. VI. Horizontal cross section of the topography and the surface wind plotted at every third grid point for the innermost LM domain for 11-10-2001 at 06:00 UTC. The wind barbs are in knots. 1: Werra valley.

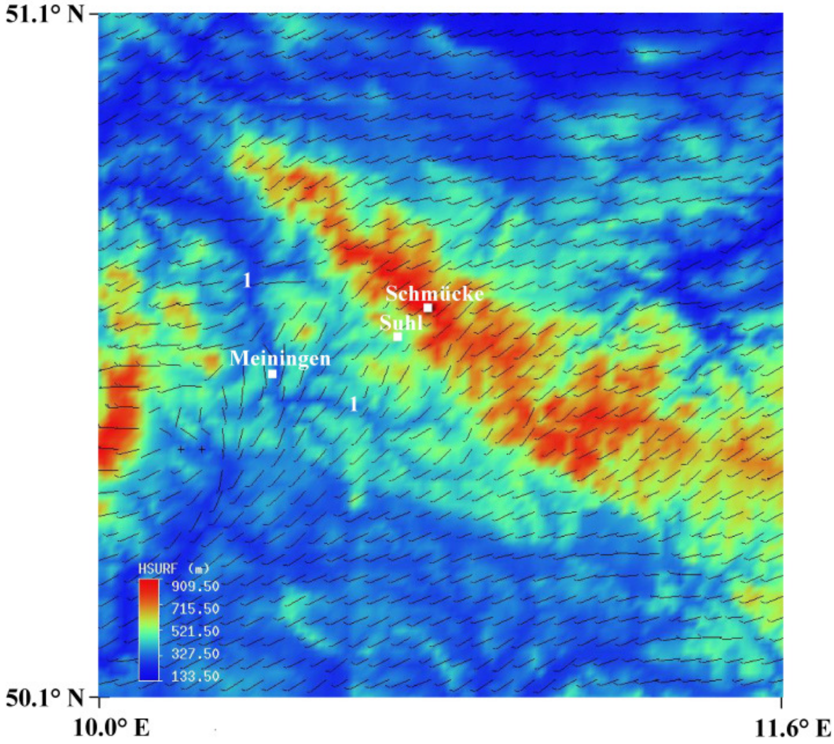

Fig. VII. Horizontal cross section of the topography and the surface wind plotted at every third grid point for the innermost LM domain for 11-10-2001 at 10:00 UTC. The wind barbs are in knots. 1: Werra valley.

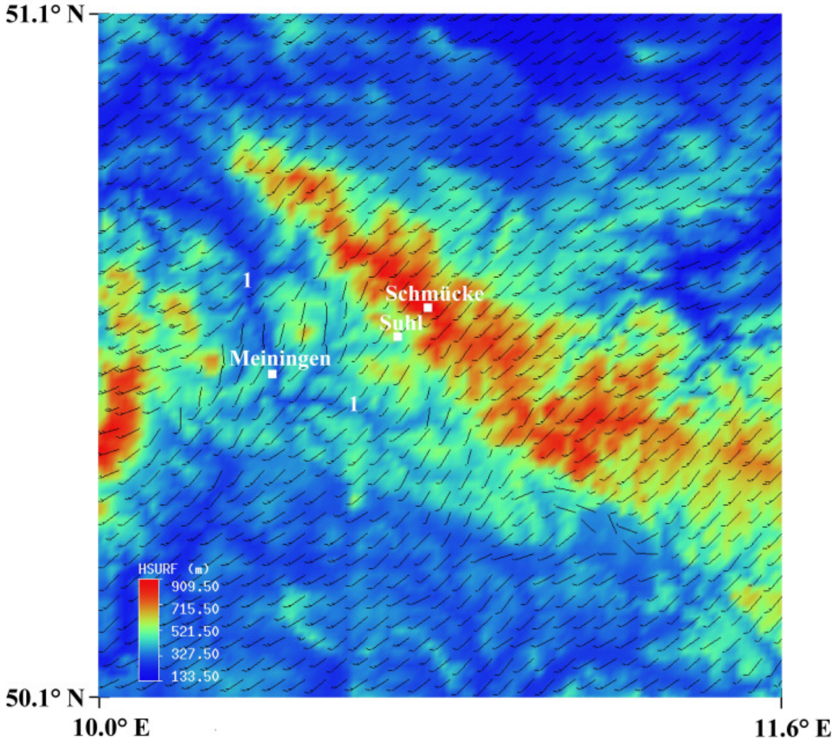

Fig. VIII. Horizontal cross section of the topography and the surface wind plotted at every third grid point for the innermost LM domain for 31-10-2001 at 10:00 UTC (tracer experiments). The wind barbs are in knots. 1: Werra valley.

Time series of the locally measured ozone for the connected flow verification (section 3.3)

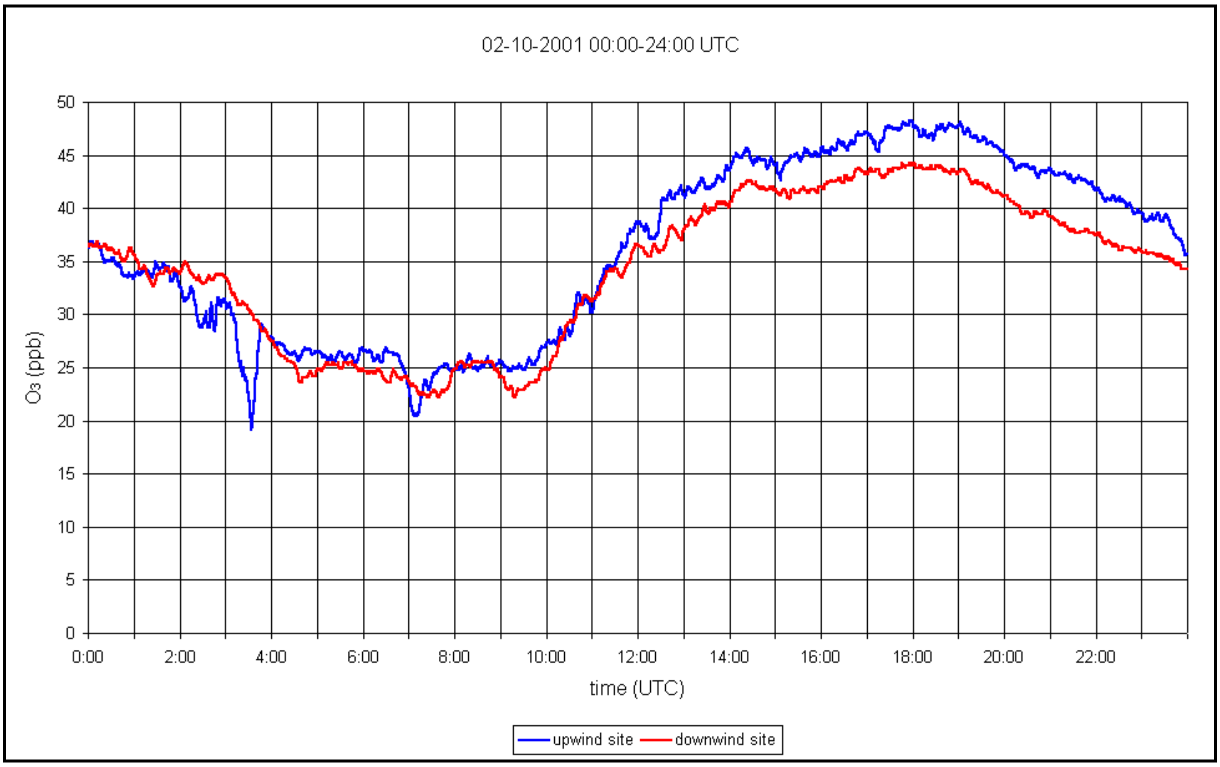

Fig. IX. Measurements of ozone at the upwind (blue line) and downwind (red line) site on 02-10-2001.

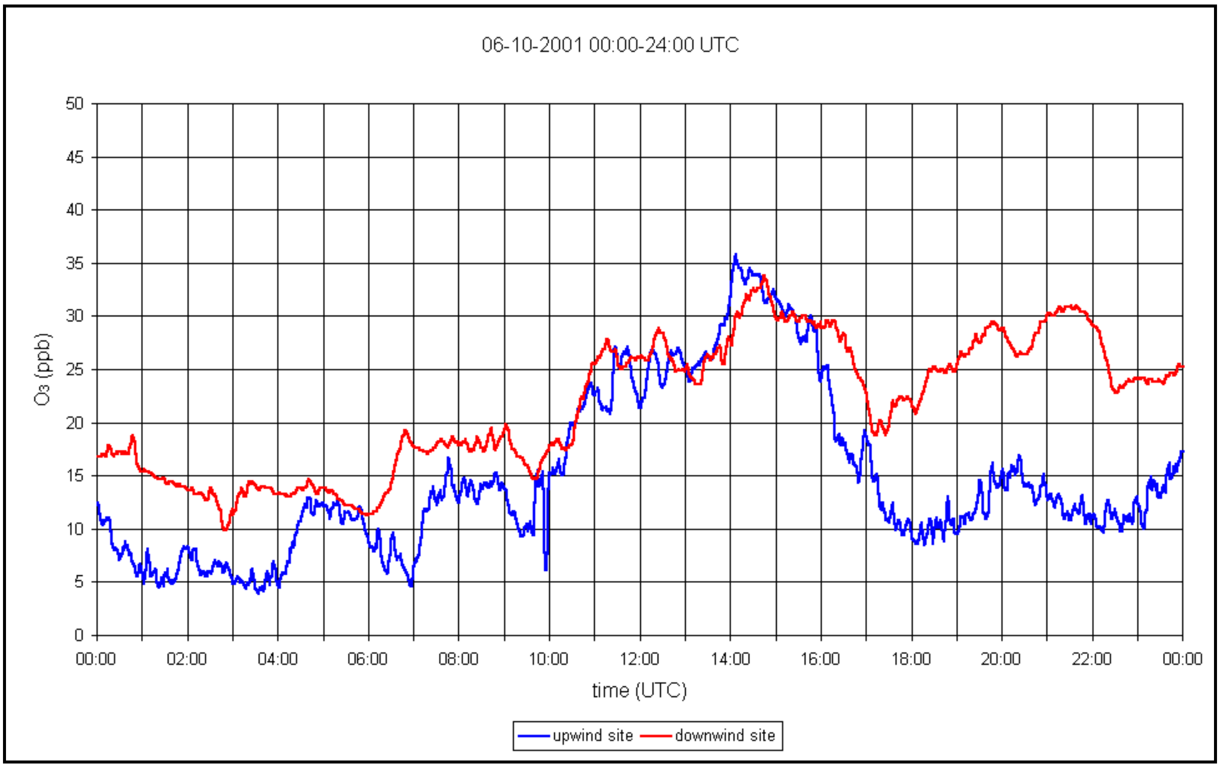

Fig. X. Measurements of ozone at the upwind (blue line) and downwind (red line) site on 06-10-2001.

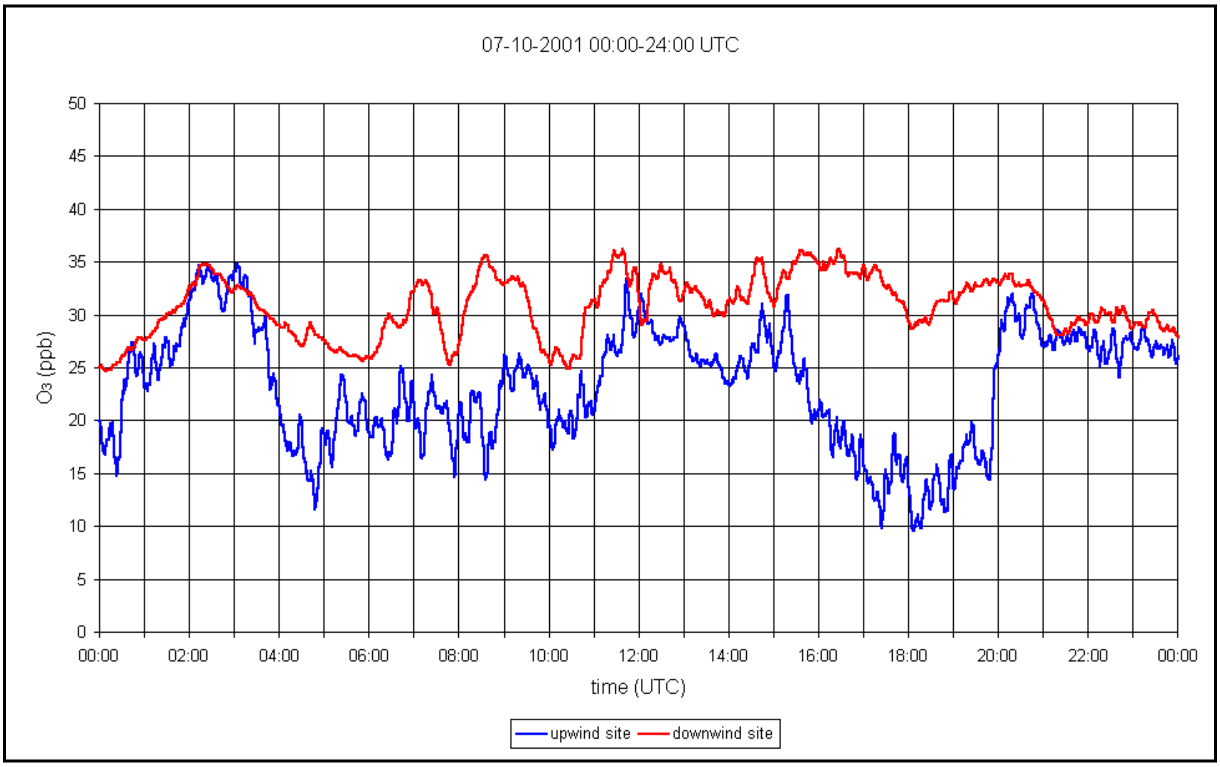

Fig. XI. Measurements of ozone at the upwind (blue line) and downwind (red line) site on 07-10-2001.

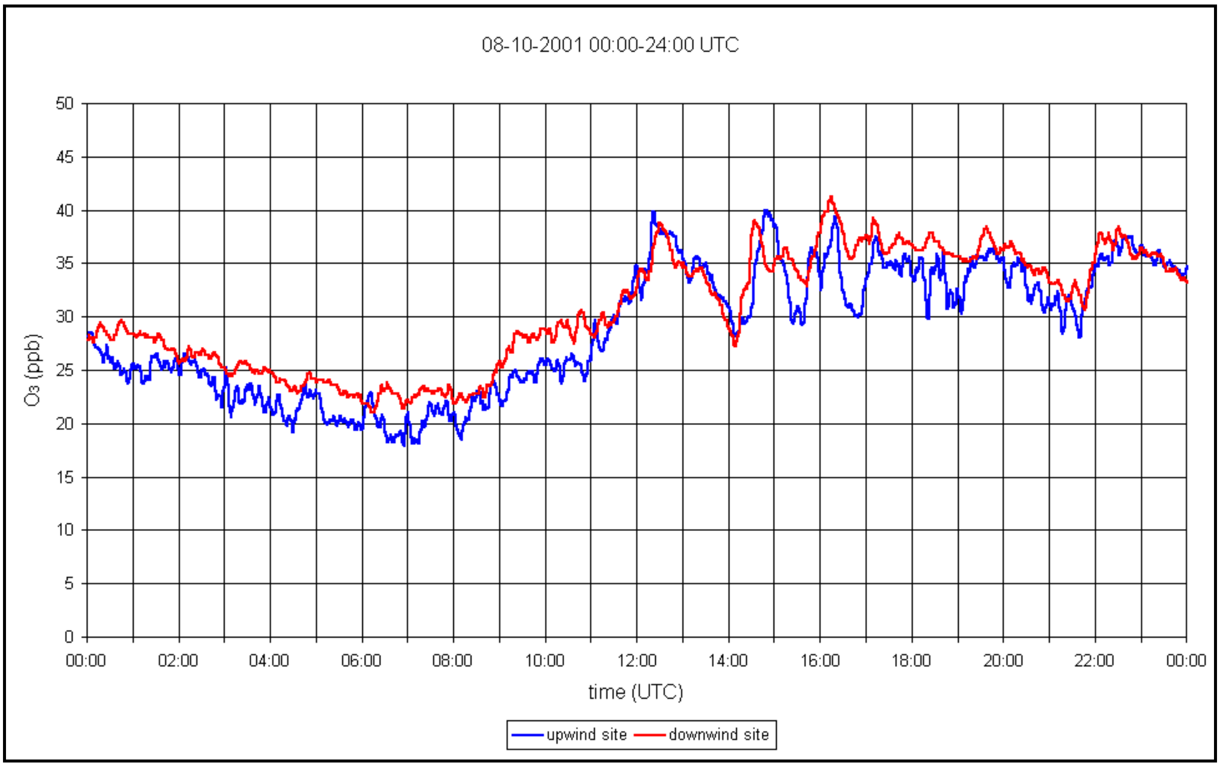

Fig. XII. Measurements of ozone at the upwind (blue line) and downwind (red line) site on 08-10-2001.

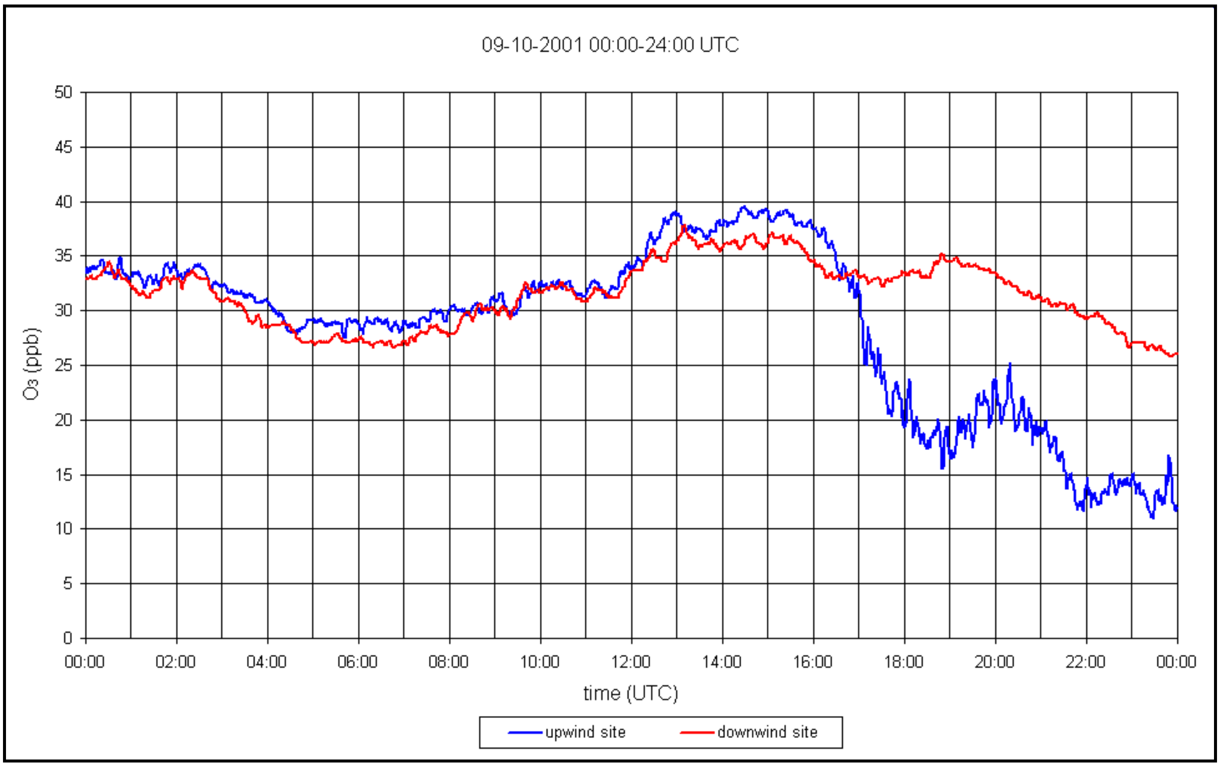

Fig. XIII. Measurements of ozone at the upwind (blue line) and downwind (red line) site on 09-10-2001.

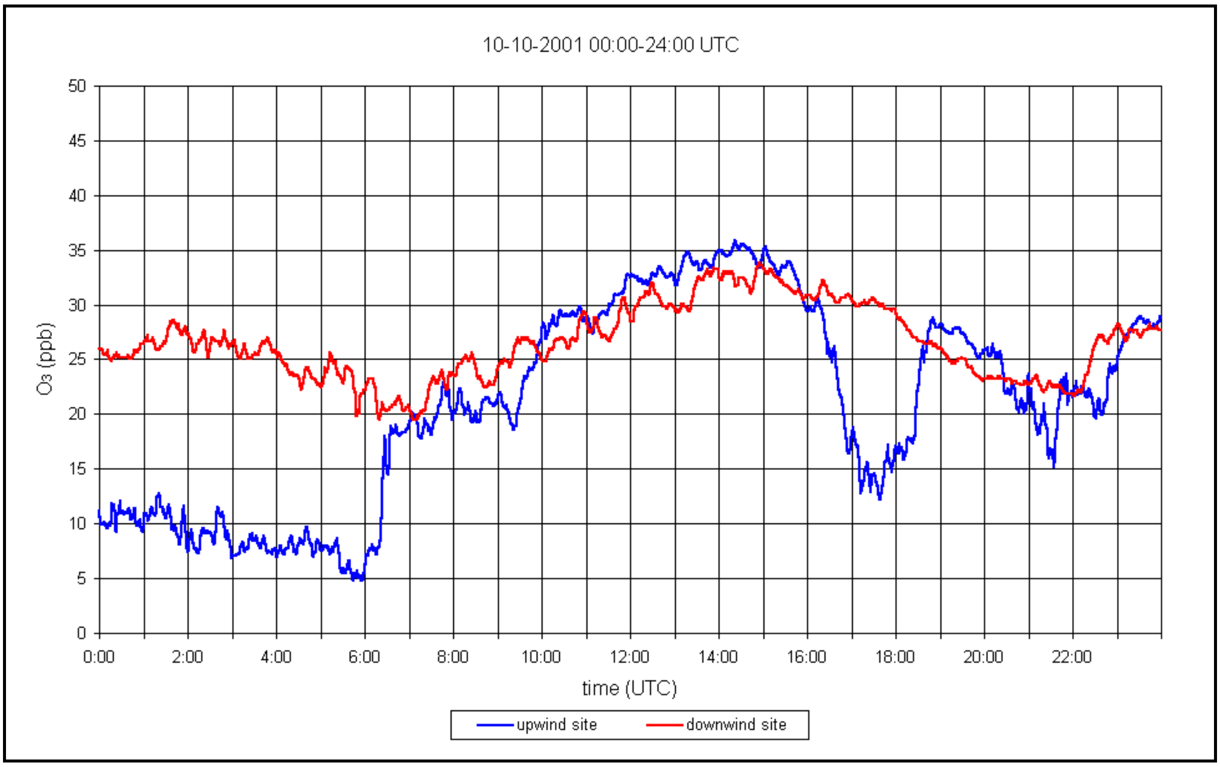

Fig. XIV. Measurements of ozone at the upwind (blue line) and downwind (red line) site on 10-10-2001.

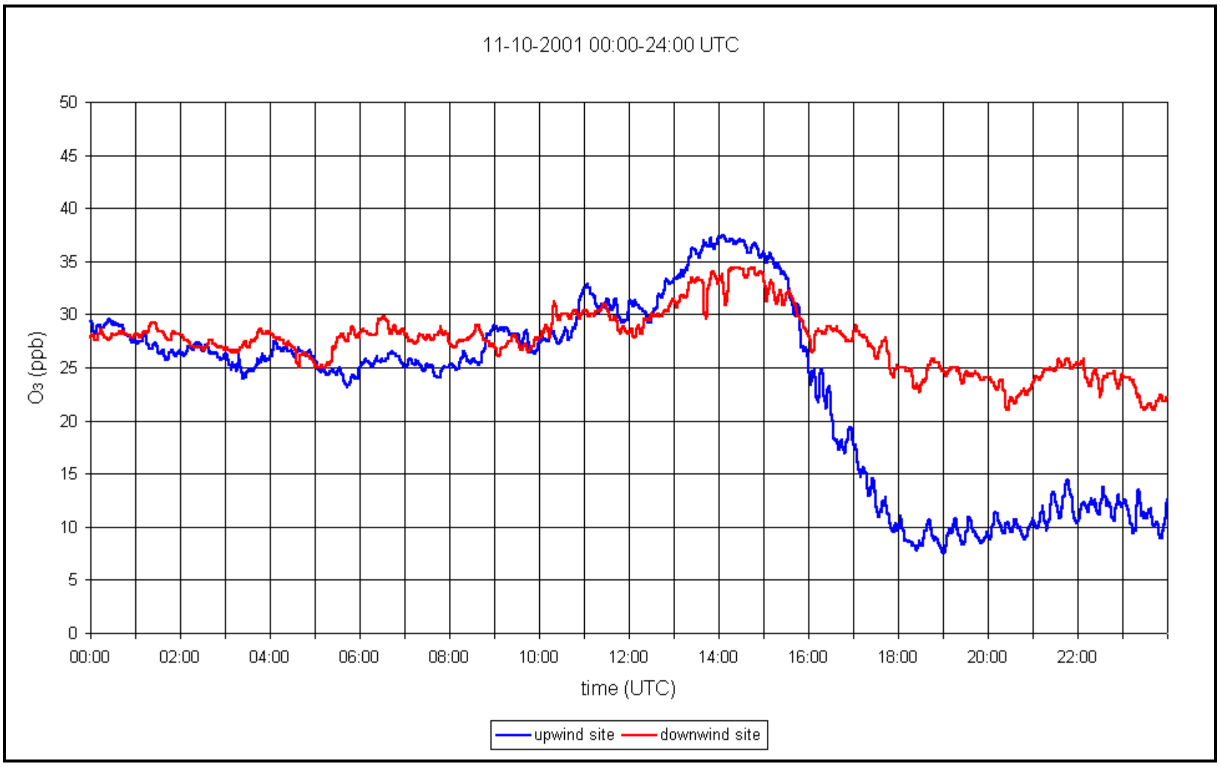

Fig. XV. Measurements of ozone at the upwind (blue line) and downwind (red line) site on 11-10-2001.

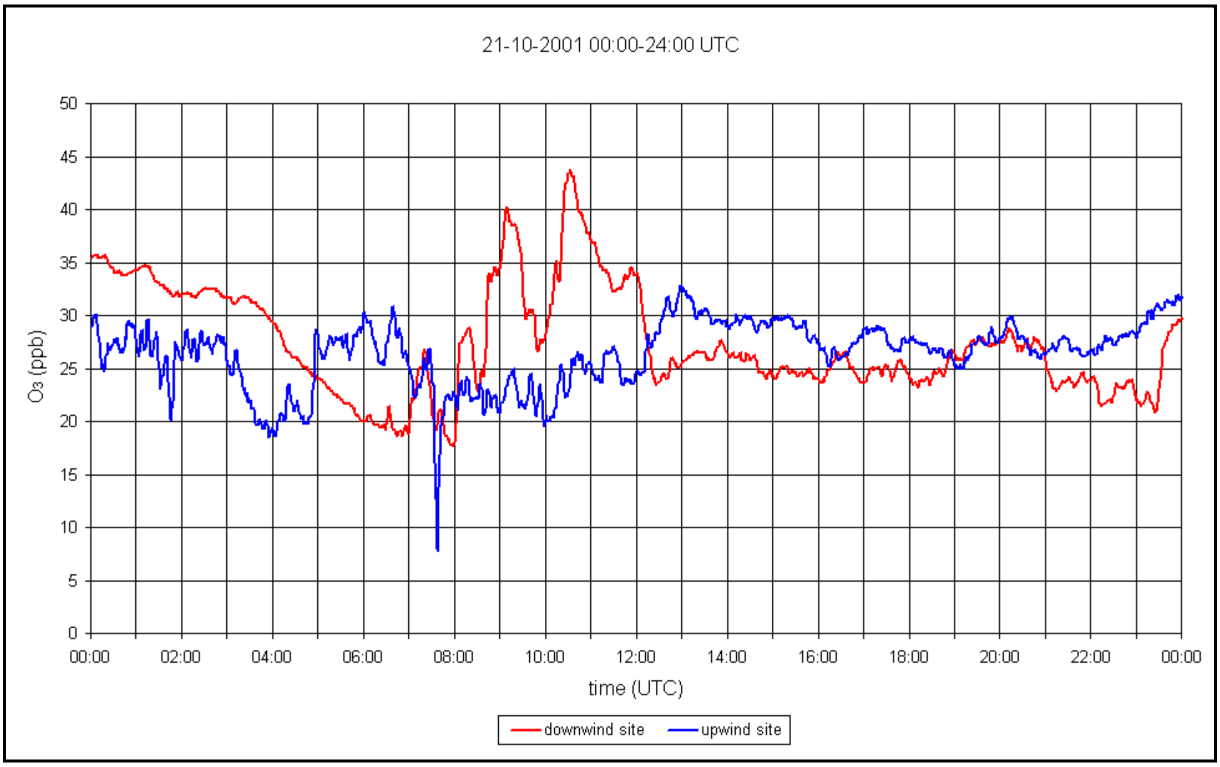

Fig. XVI. Measurements of ozone at the upwind (blue line) and downwind (red line) site on 21-10-2001.

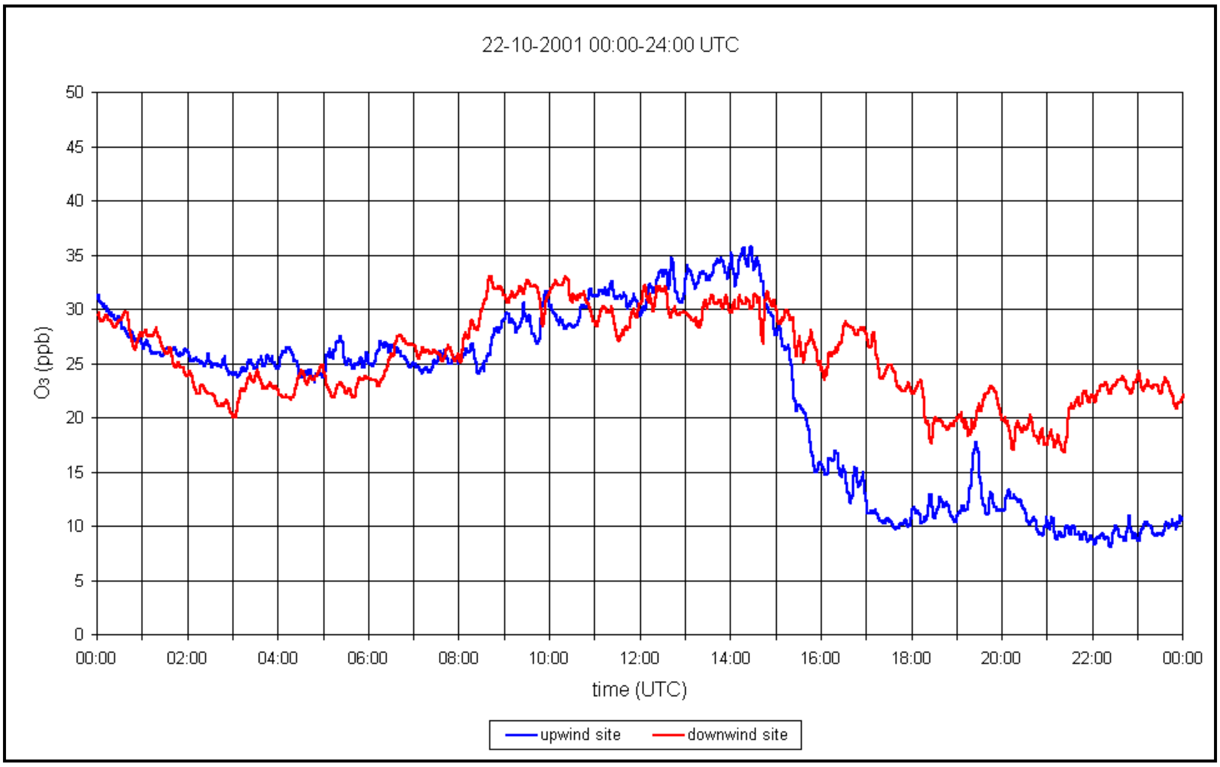

Fig. XVII. Measurements of ozone at the upwind (blue line) and downwind (red line) site on 22-10-2001.

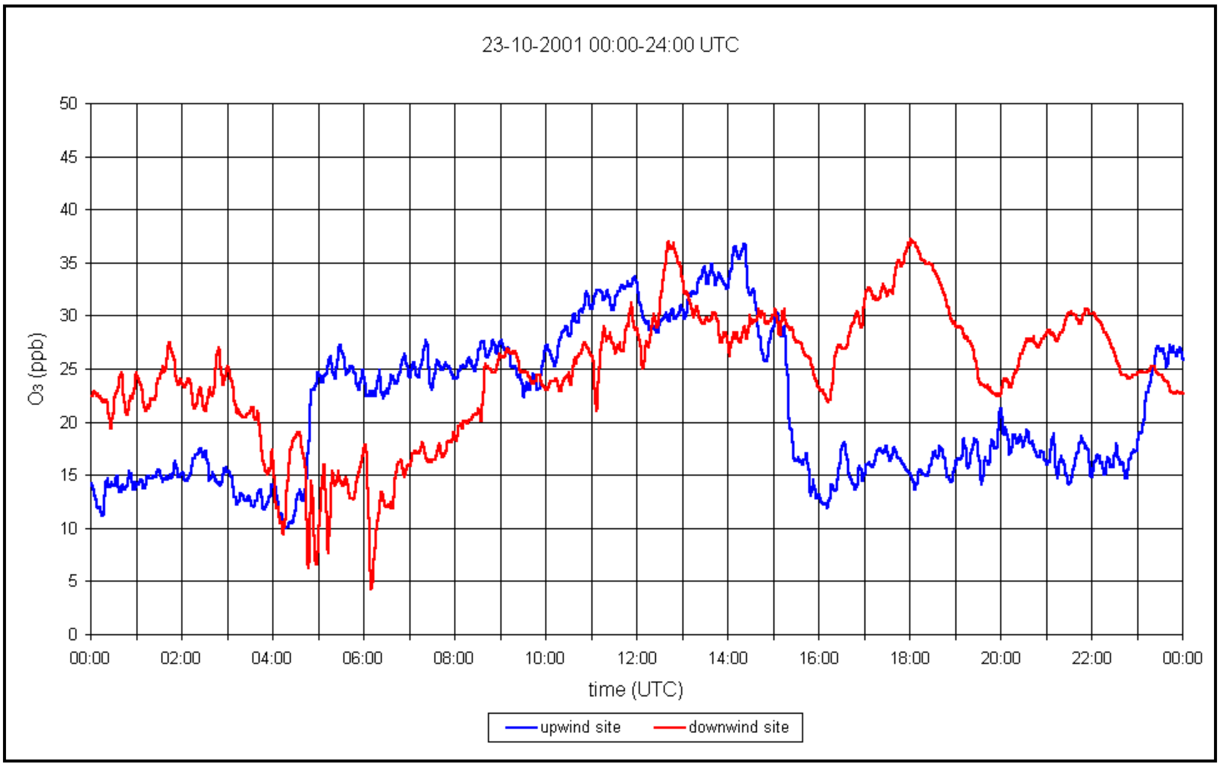

Fig. XVIII. Measurements of ozone at the upwind (blue line) and downwind (red line) site on 23-10-2001.

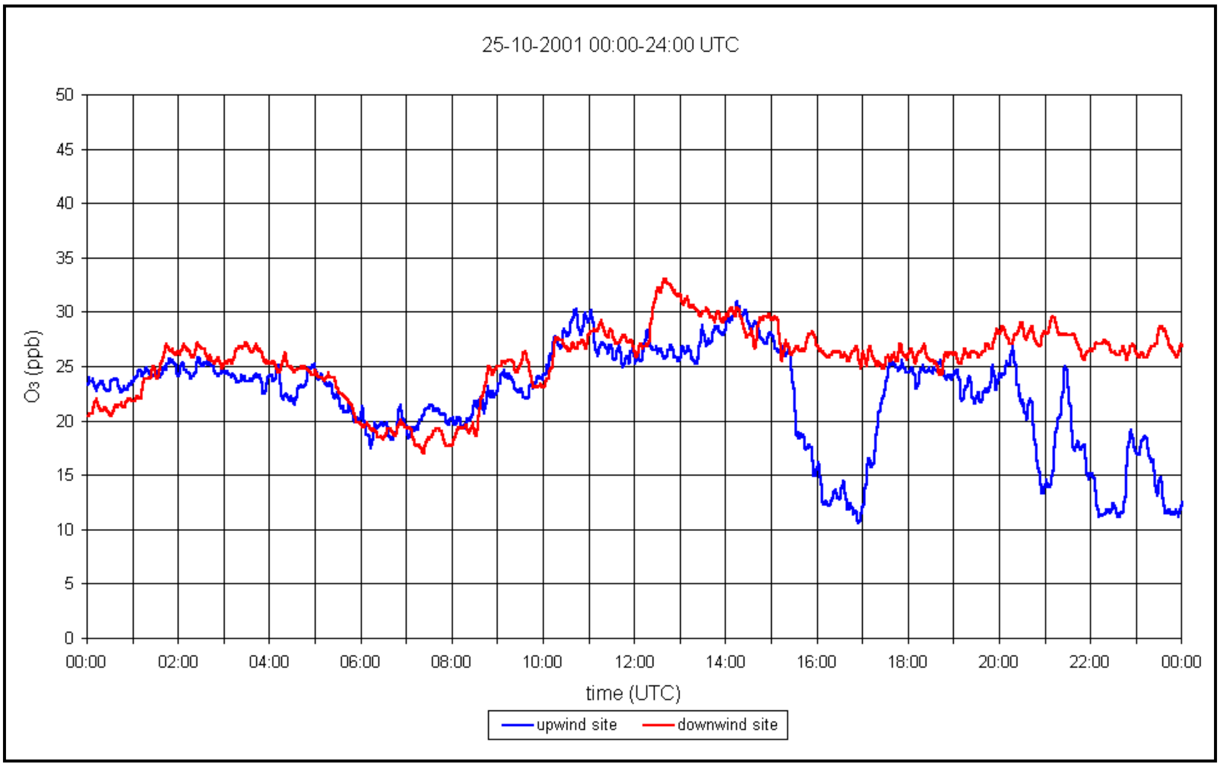

Fig. XIX. Measurements of ozone at the upwind (blue line) and downwind (red line) site on 25-10-2001.

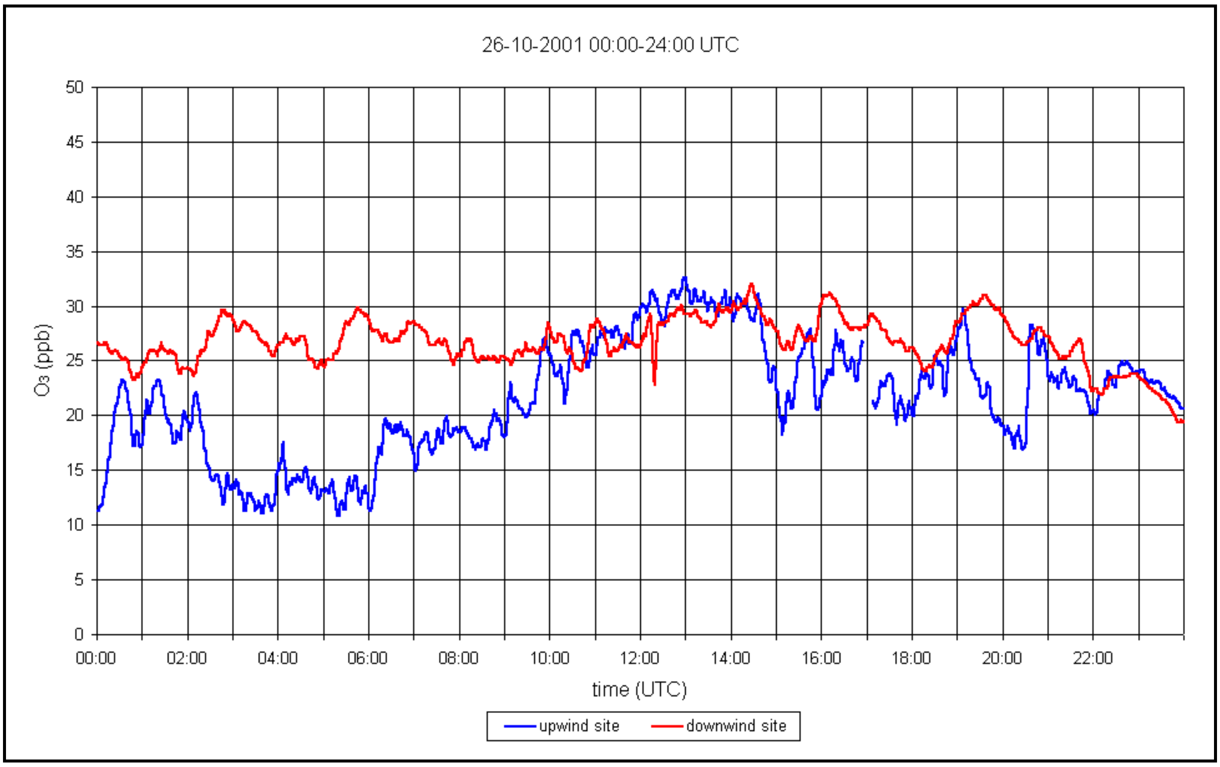

Fig. XX. Measurements of ozone at the upwind (blue line) and downwind (red line) site on 26-10-2001.

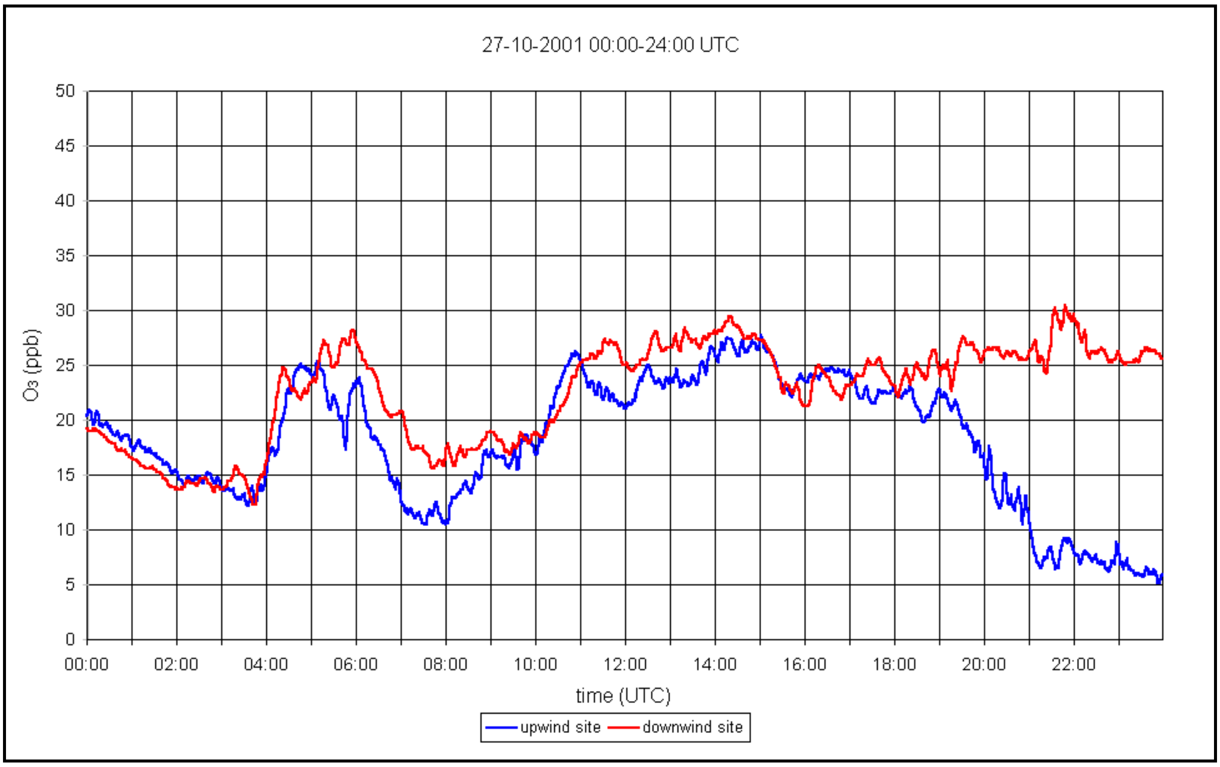

Fig. XXI. Measurements of ozone at the upwind (blue line) and downwind (red line) site on 27-10-2001.

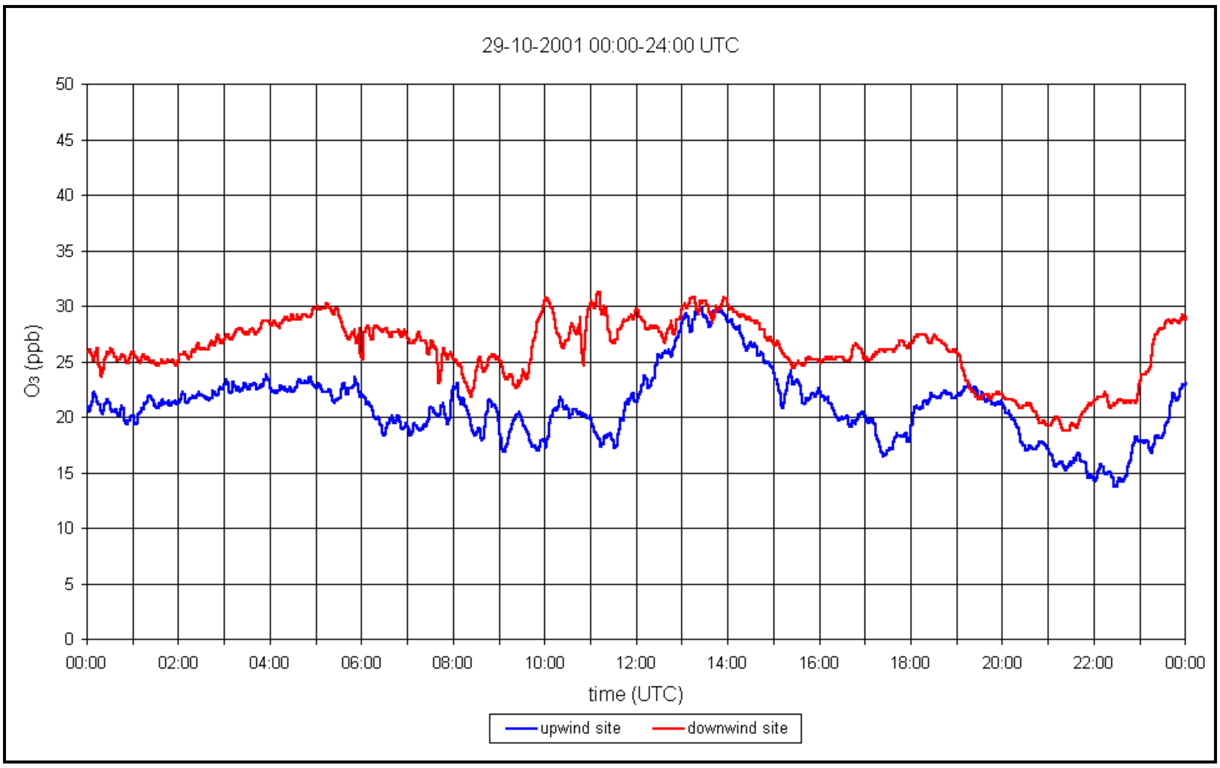

Fig. XXII. Measurements of ozone at the upwind (blue line) and downwind (red line) site on 29-10-2001.

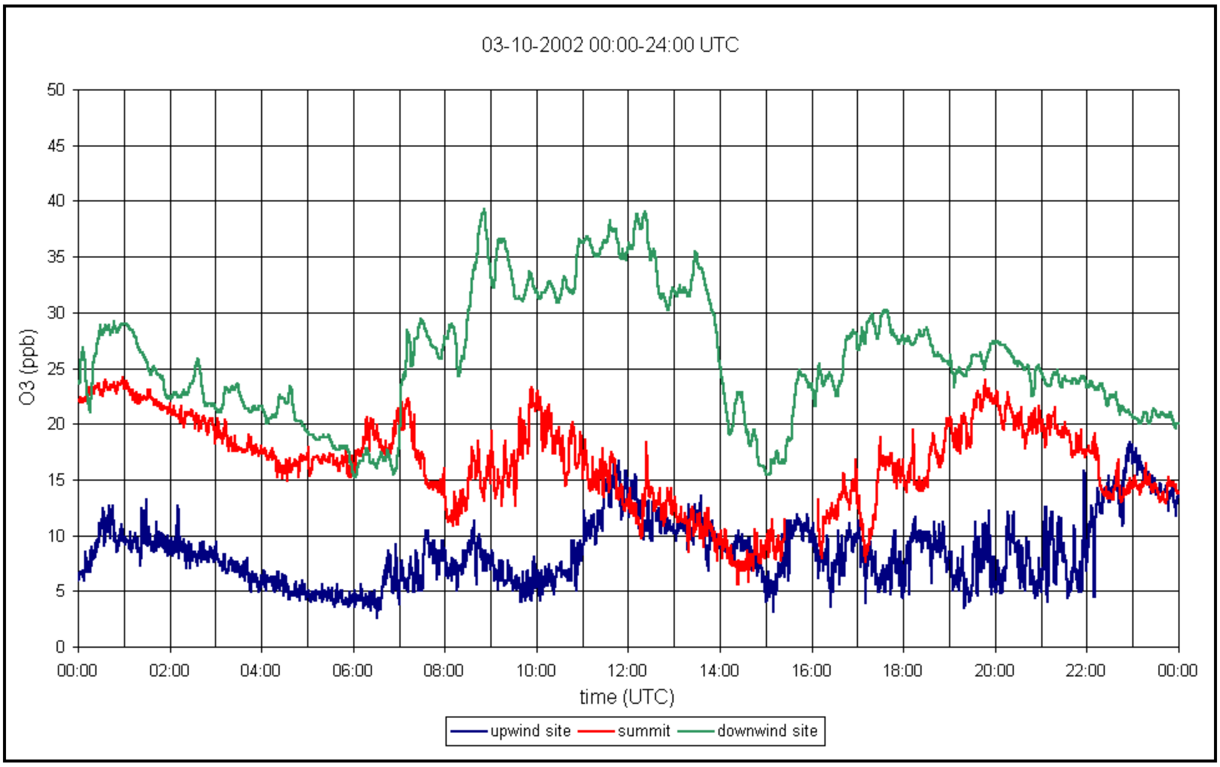

Fig. XXIII. Measurements of ozone at the upwind site (blue line), summit (red line) and downwind (green line) site on 03-10-2002.

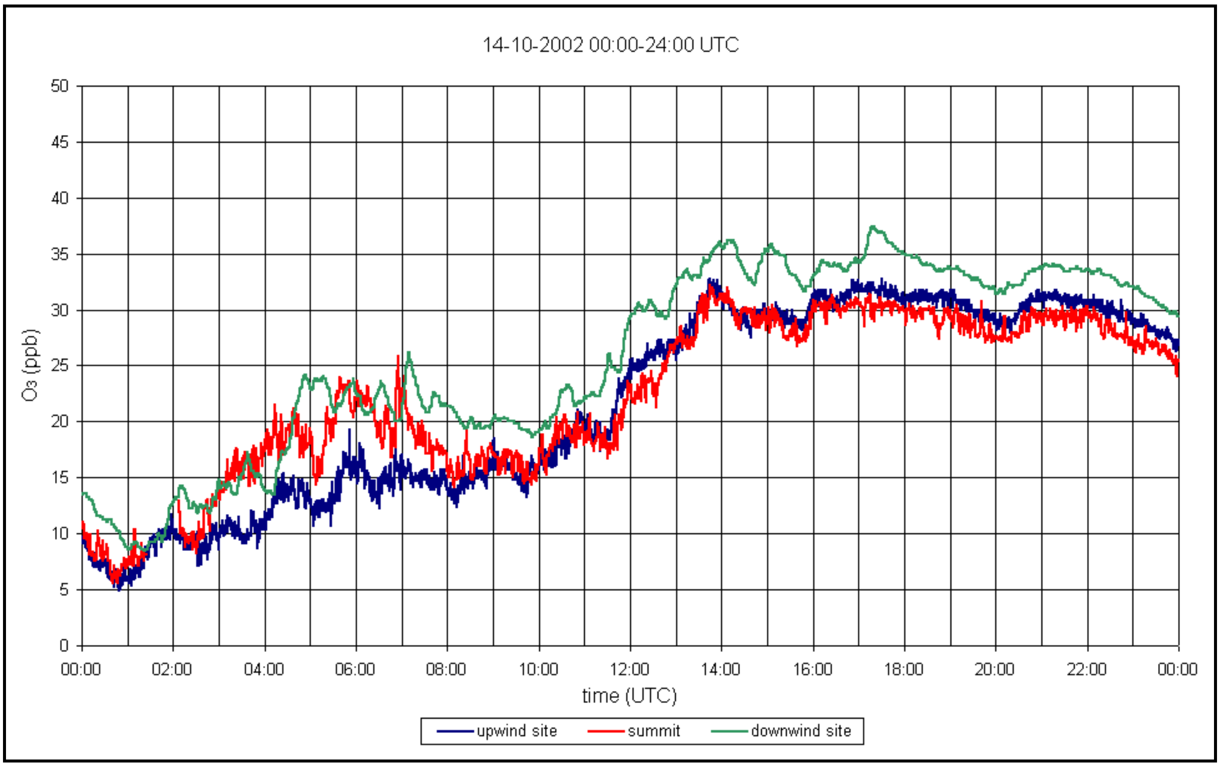

Fig. XXIV. Measurements of ozone at the upwind site (blue line), summit (red line) and downwind (green line) site on 14-10-2002.

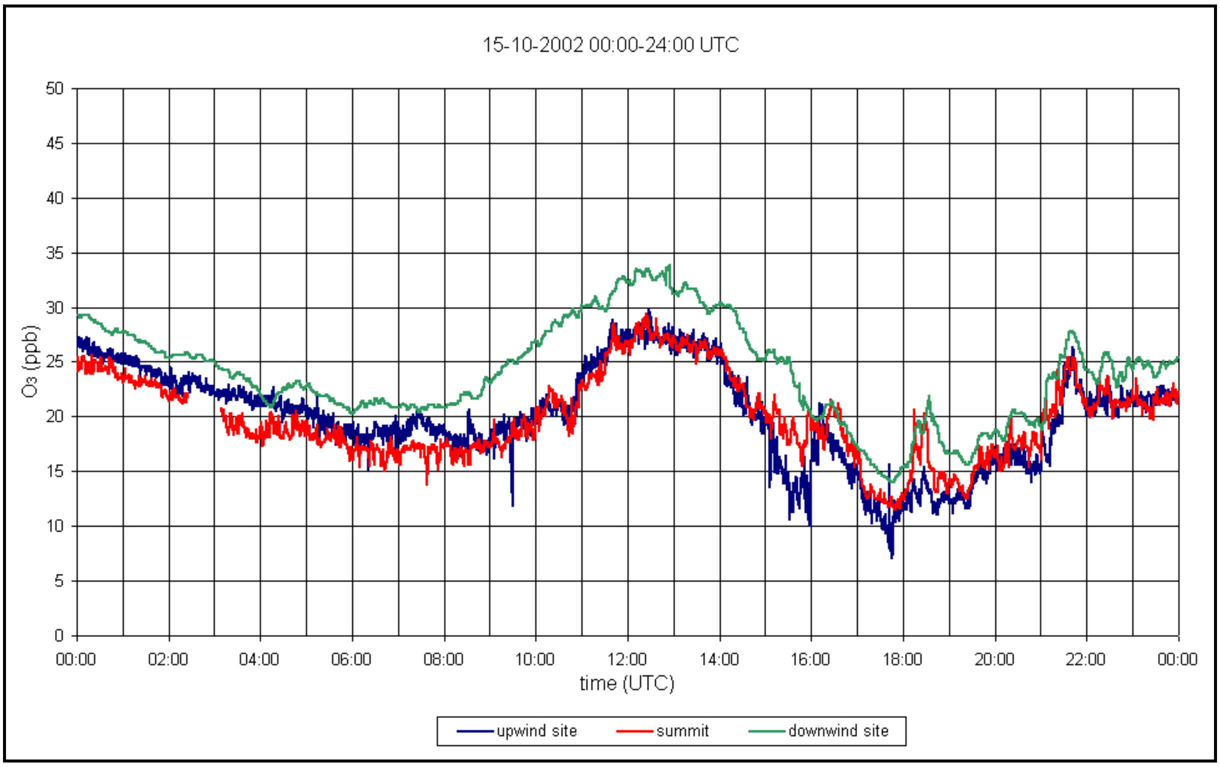

Fig. XXV. Measurements of ozone at the upwind site (blue line), summit (red line) and downwind (green line) site on 15-10-2002.

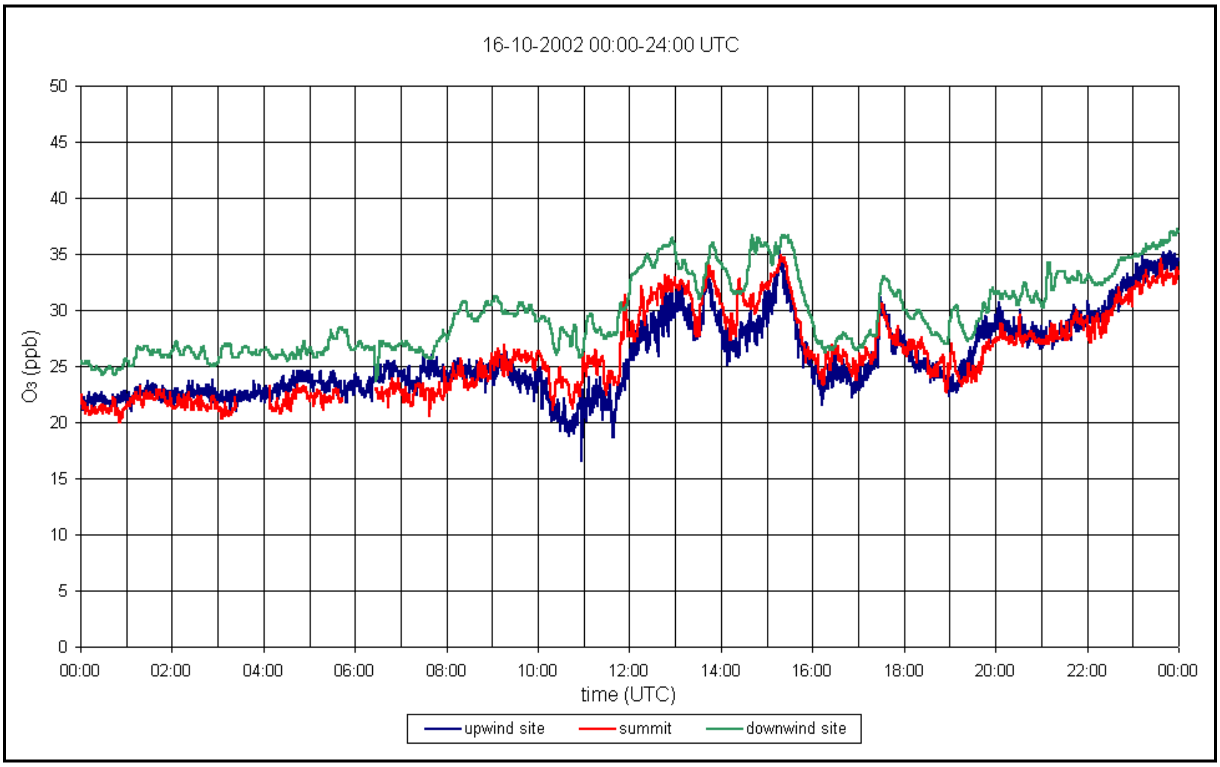

Fig. XXVI. Measurements of ozone at the upwind site (blue line), summit (red line) and downwind (green line) site on 16-10-2002.

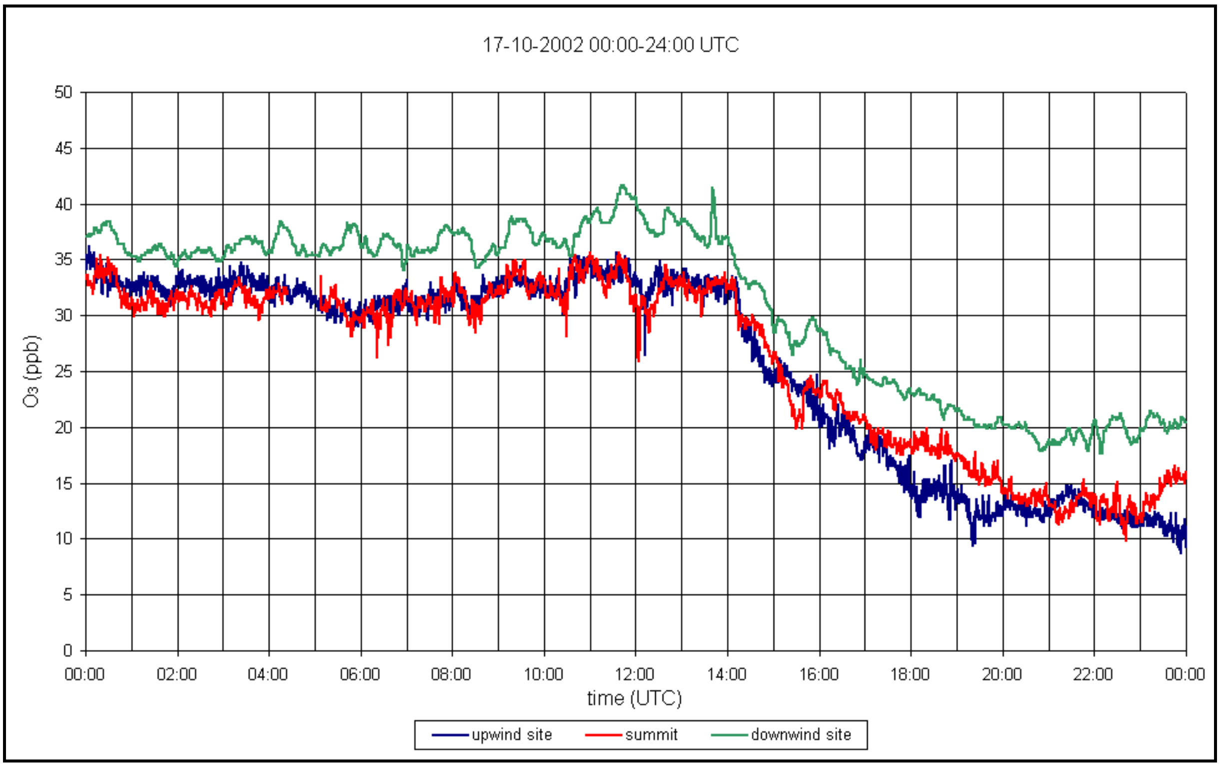

Fig. XXVII. Measurements of ozone at the upwind site (blue line), summit (red line) and downwind (green line) site on 17-10-2002.

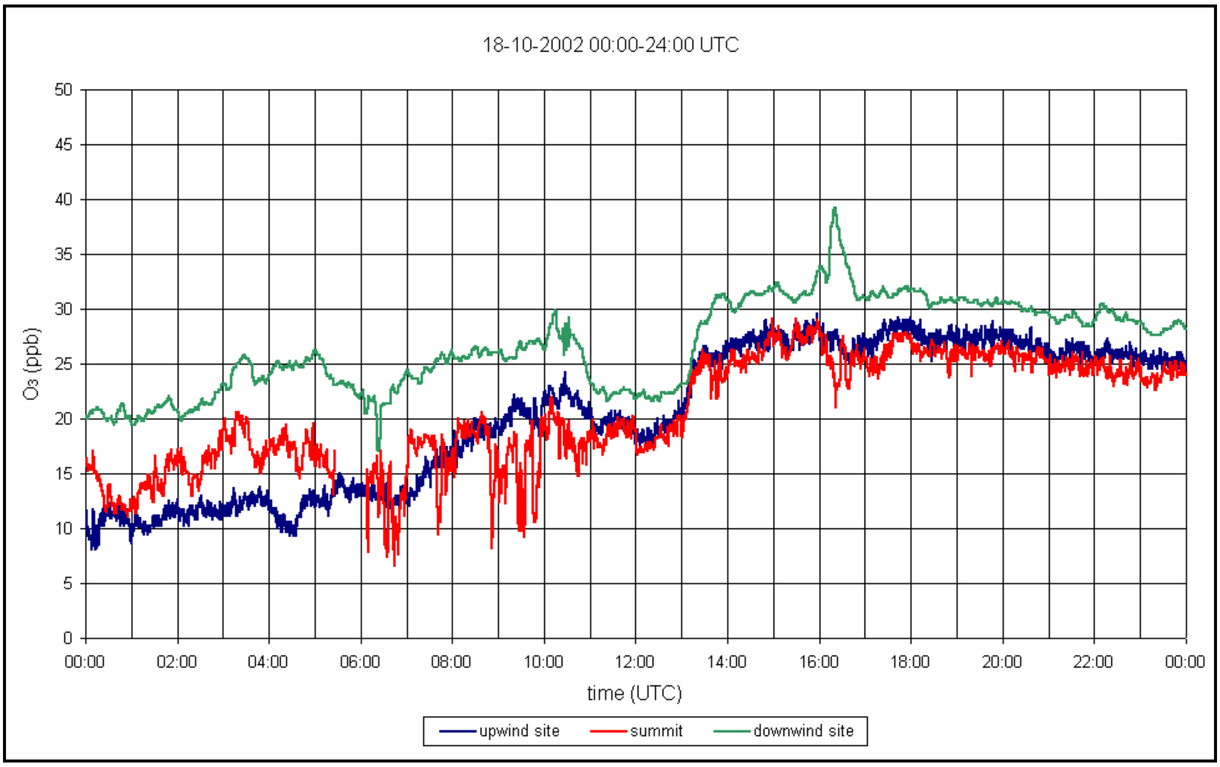

Fig. XXVIII. Measurements of ozone at the upwind site (blue line), summit (red line) and downwind (green line) site on 18-10-2002.

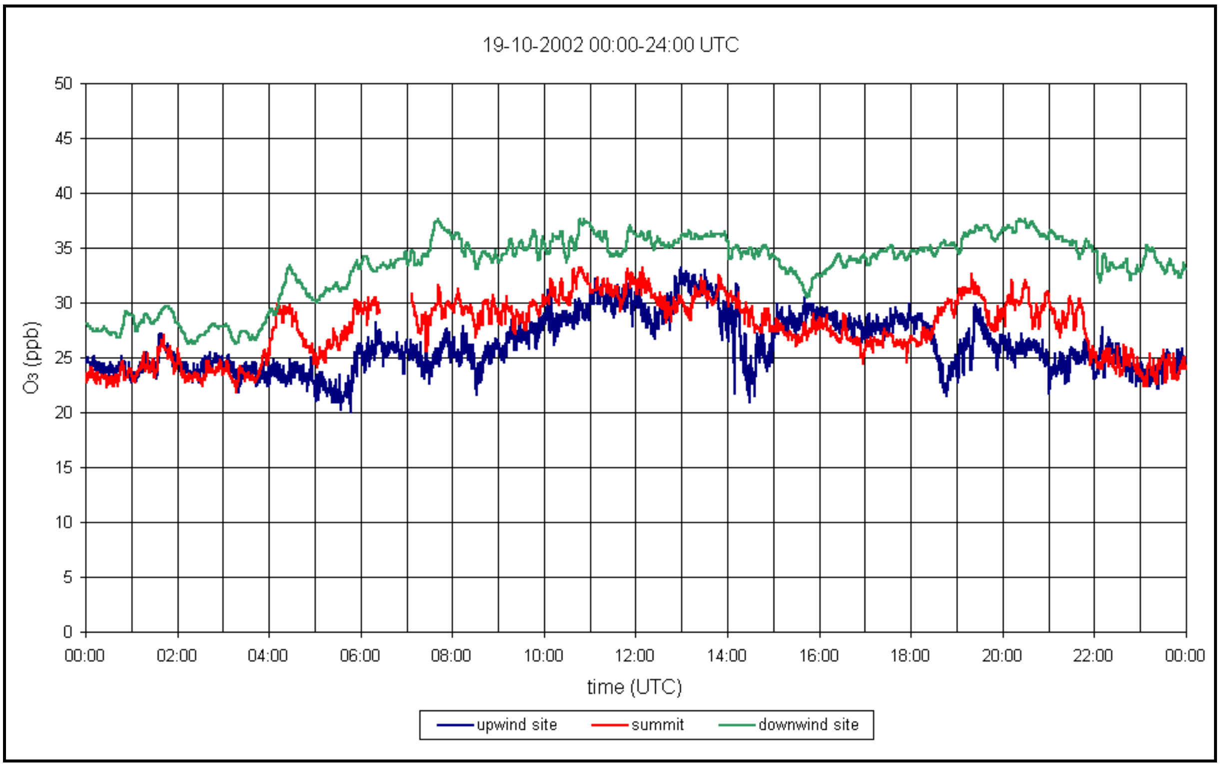

Fig. XXIX. Measurements of ozone at the upwind site (blue line), summit (red line) and downwind (green line) site on 19-10-2002.

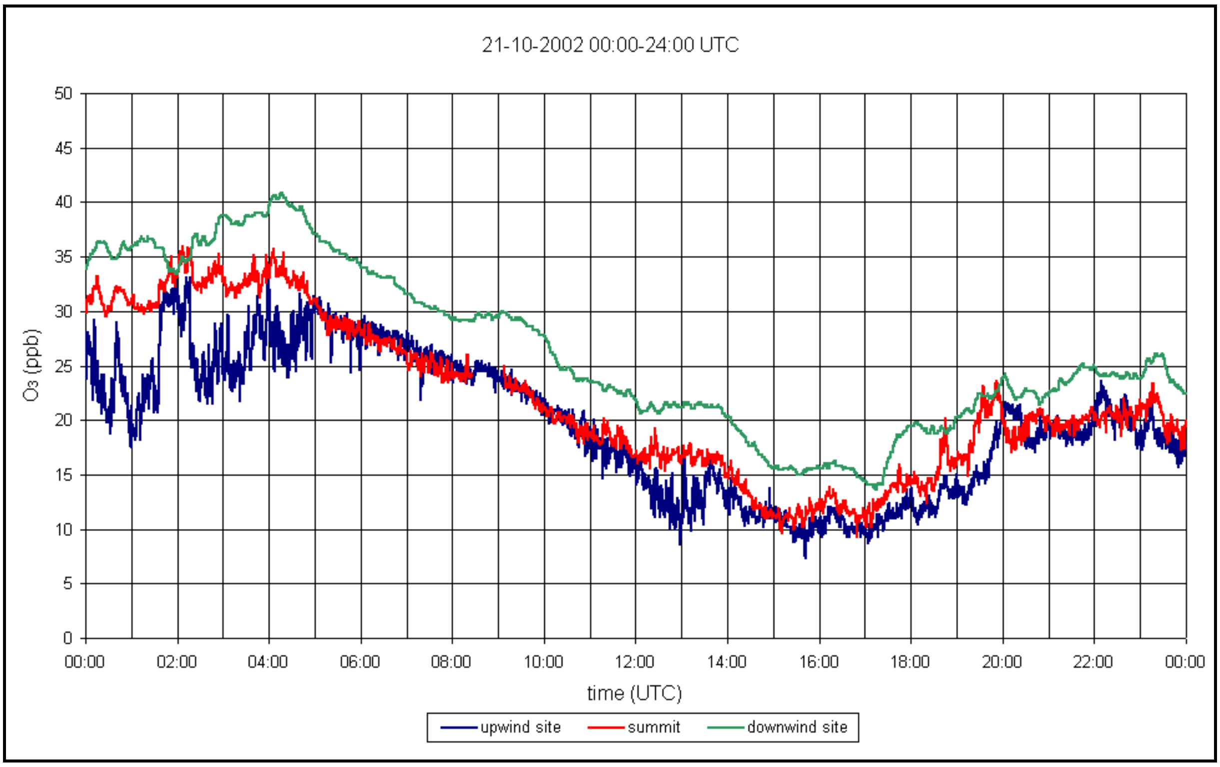

Fig. XXX. Measurements of ozone at the upwind site (blue line), summit (red line) and downwind (green line) site on 21-10-2002.

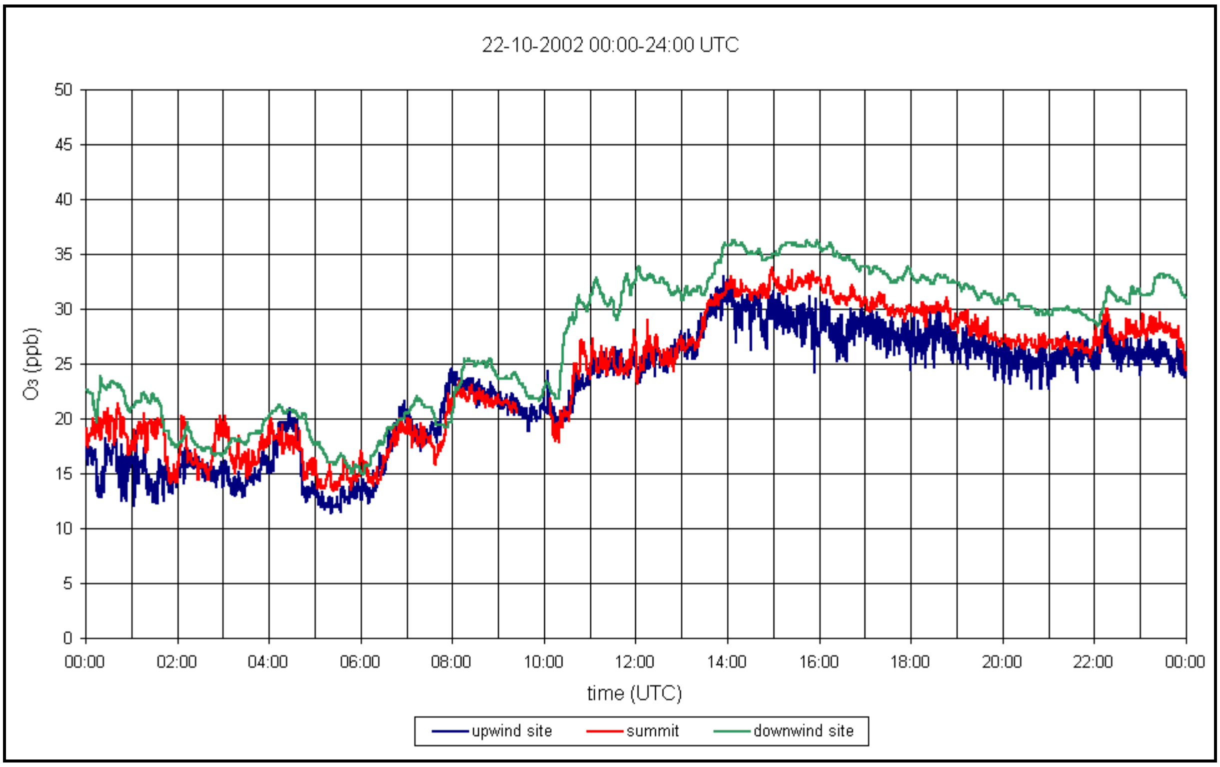

Fig. XXXI. Measurements of ozone at the upwind site (blue line), summit (red line) and downwind (green line) site on 22-10-2002.

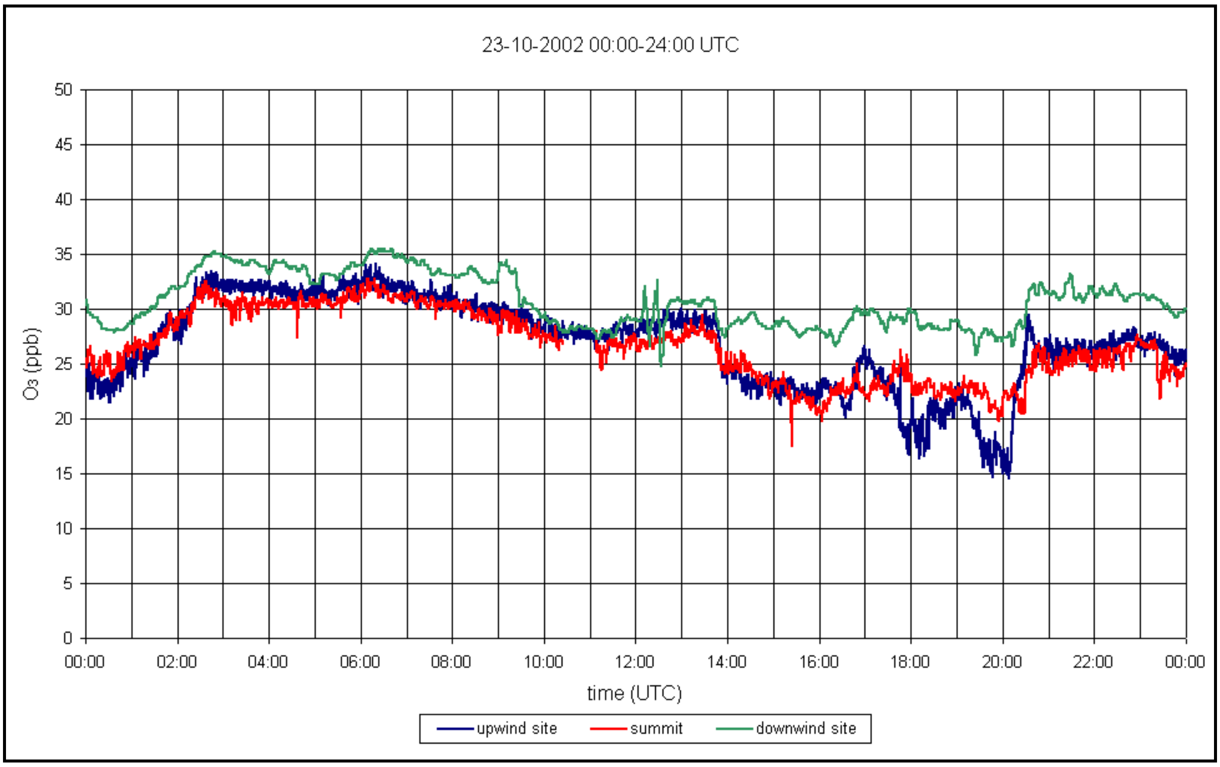

Fig. XXXII. Measurements of ozone at the upwind site (blue line), summit (red line) and downwind (green line) site on 23-10-2002.

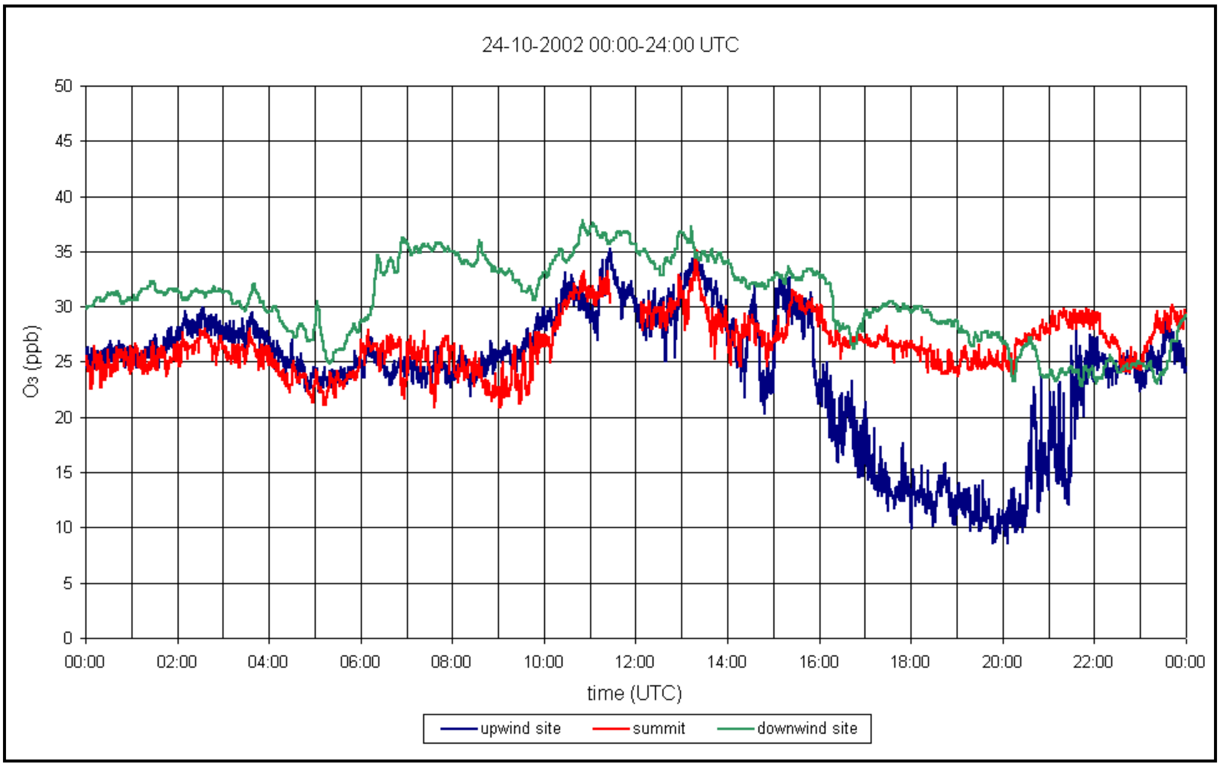

Fig. XXXIII. Measurements of ozone at the upwind site (blue line), summit (red line) and downwind (green line) site on 24-10-2002.

Results of SF_6 tracer experiments and simulations not presented in the text (section 3.4)

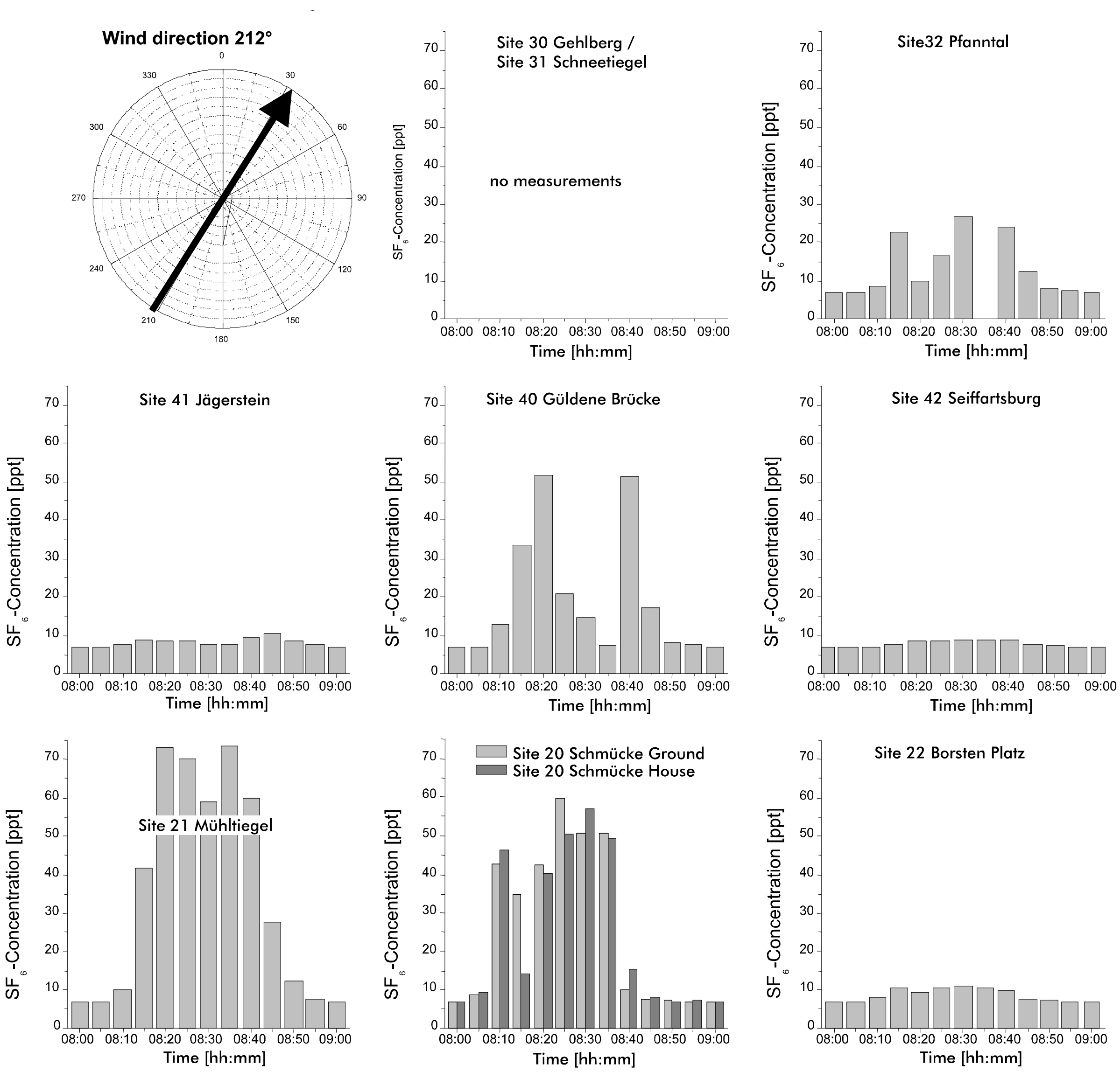

Fig. XXXIV. Time series of SF_6 concentrations (ppt) at different receptor sites on 16-05-2001.

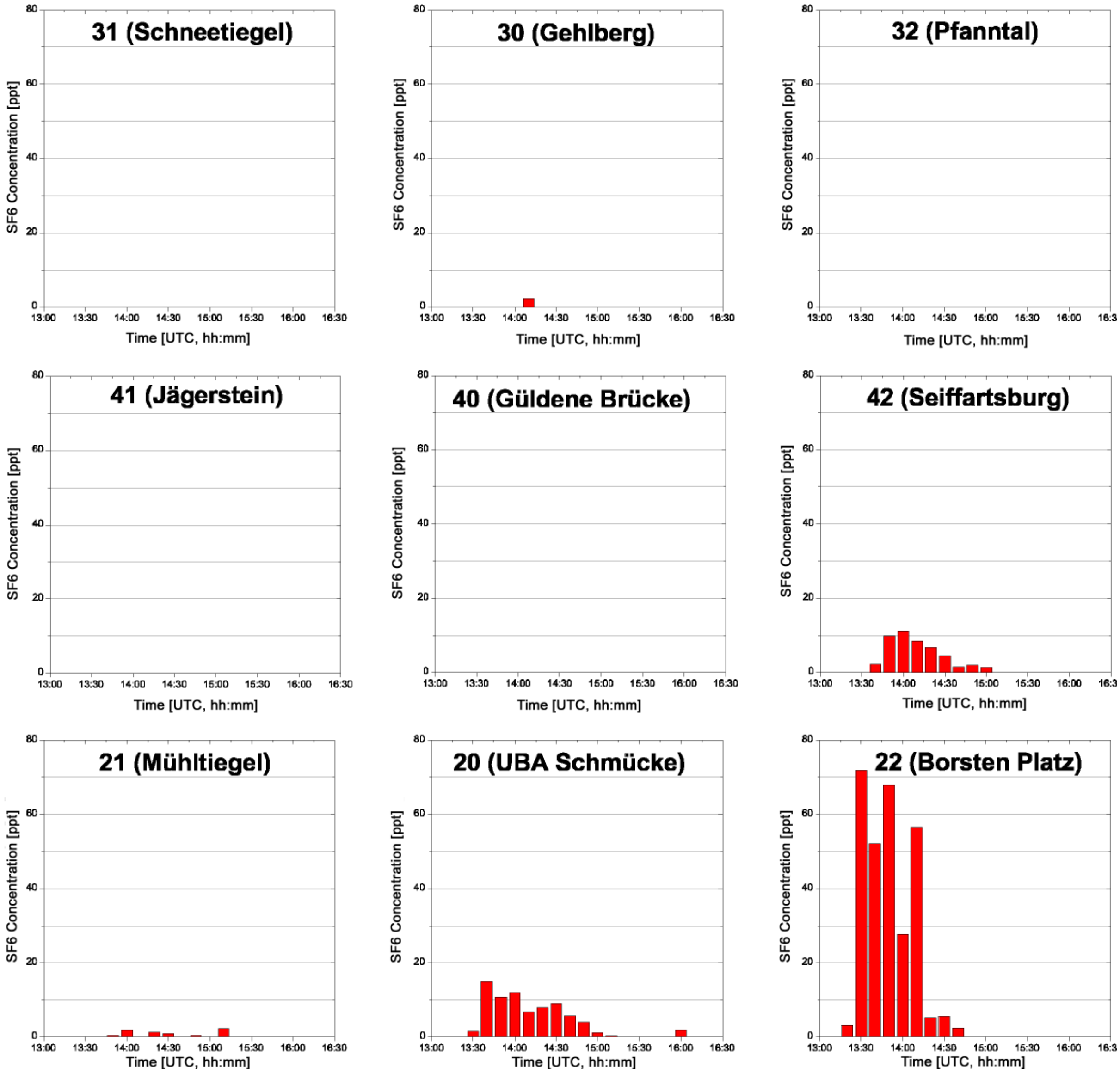

Fig. XXXV. Time series of SF_6 concentrations (ppt) at different receptor sites on 18-05-2001.

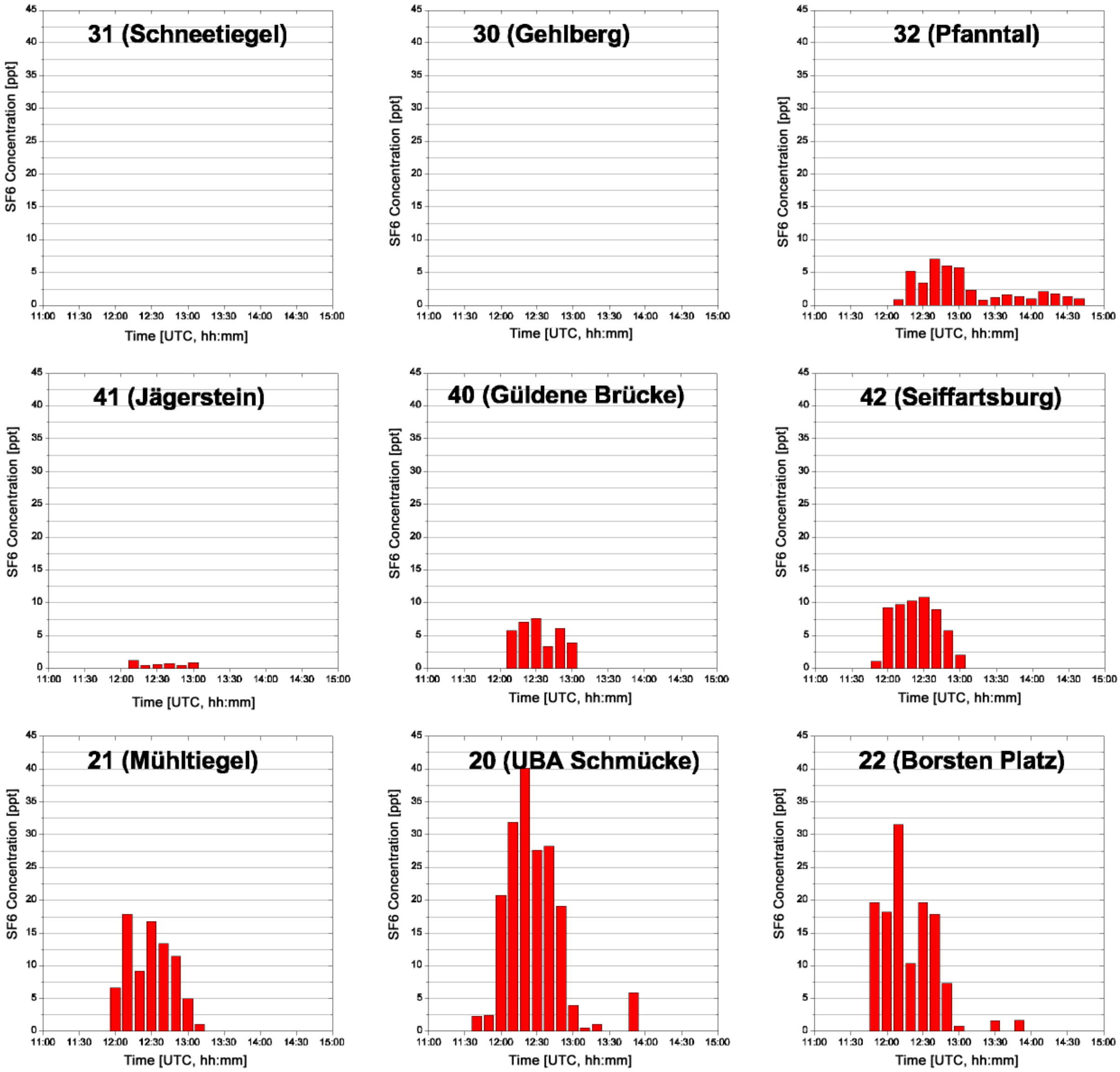

Fig. XXXVI. Time series of SF_6 concentrations (ppt) at different receptor sites on 07-06-2001.

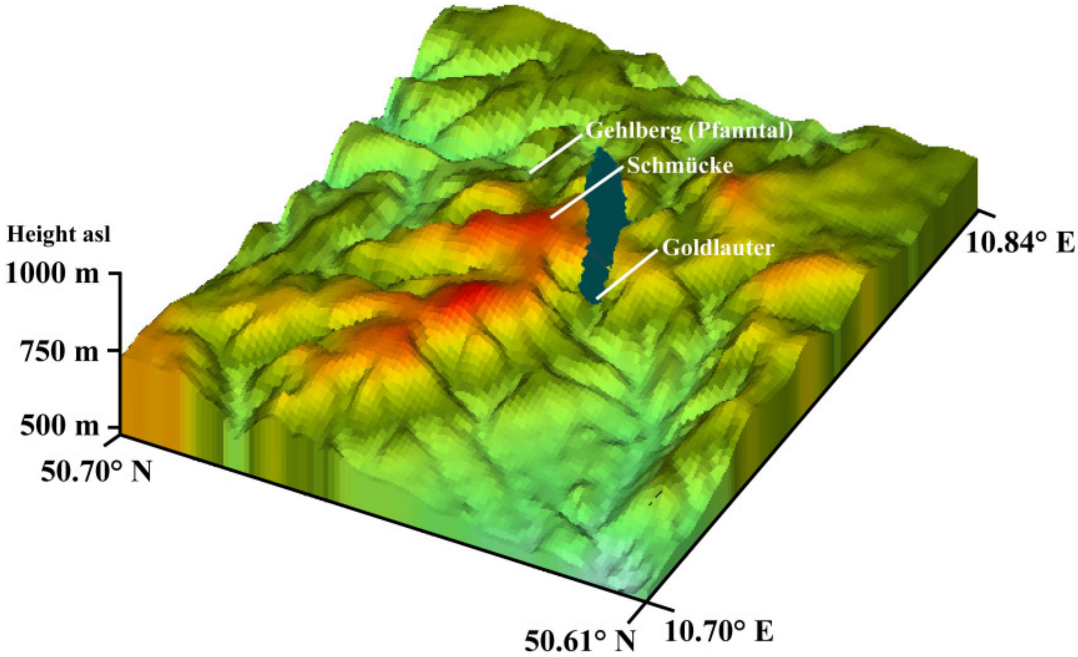

Fig. XXXVII. Topography and isovolume plot of the simulated (ASAM) SF_6 concentration greater than 25 ppt for 31-10-2001 at 09:20 UTC (20 minutes after the beginning of tracer release).

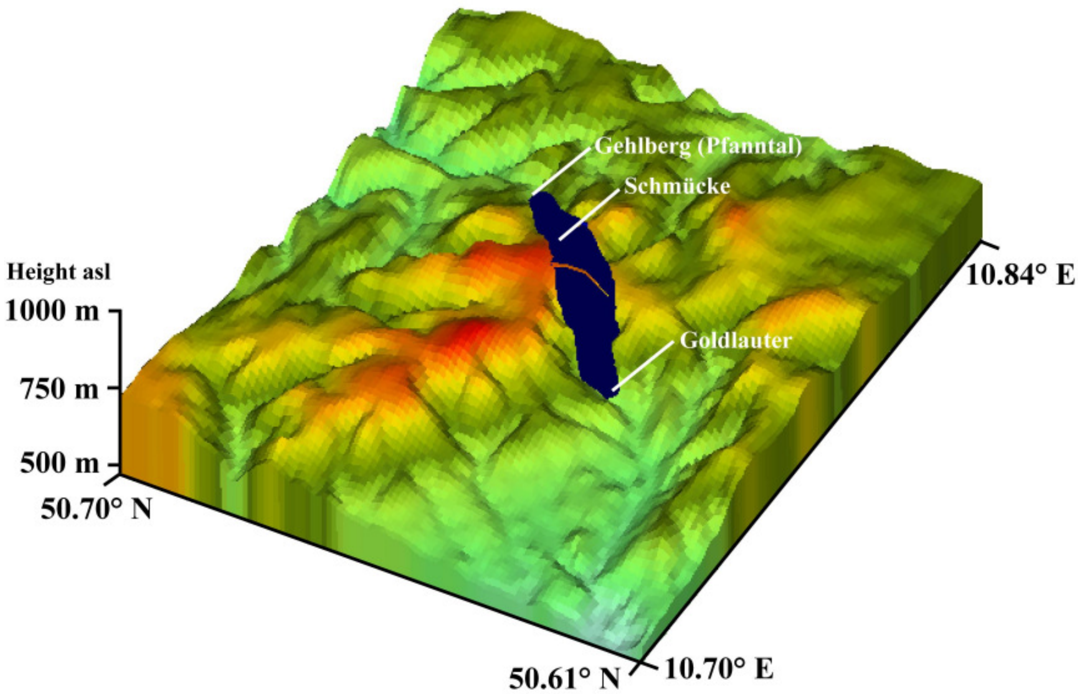

Fig. XXXVIII. Topography and isovolume plot of the simulated (ASAM) SF_6 concentration greater than 35 ppt for 16-10-2002 at 08:20 UTC (20 minutes after the beginning of tracer release).

Final event classification (section 4)

Table I. Event classification of six pre-selected FEBUKO cloud events in 2001 and 2002 based on flow characterisation. These events were chosen out of 14 cloud episodes due to most adequate synoptical conditions.

Priority	**Date**	**Remarks**	
		Synoptical conditions/ completeness of data set (Tilgner et al., 2005)	**Mesoscale and local flow**
E1	26/27 Oct. 2001	Stable south-westerly flow conditions, low stratus, longest undivided event	***LM:*** Weakening orographic effects, zone of southwesterly flow over the mid mountain range, only little blocking effects from 09 UTC on 27 October, gravity waves ***Froude number:*** Weakening deceleration (Fr = 1.22/0.81) ***Ozone:*** Especially in the middle of the event minor differences between the ozone profiles
E2	06-08 Oct. 2001	Stable south-westerly flow and cloud conditions in the last dominant section	***LM:*** On 6/7 October blocking, low wind speeds and air passing around the ridge, but increased wind speeds and flow over the mountain range from southwest during the last and longest section on 8 October ***Froude number:*** minor or no deceleration in the last section (8-10-2001: Fr = 0.96/0.36) ***Ozone:*** Approximately the same ozone profiles at all sites at least on 8 October
E3	16/17 Oct. 2002	Particularly adequate flow characteristics (high wind speed and constant from southwest), sufficient experimental time, stratus cloud	***LM:*** Less complex flow pattern, high wind speeds up to 10 m s^{-1}, only minor channelling in the Werra valley, neglecting upwind deceleration ***Froude number:*** Minor or no deceleration ($0.26 \leq$ Fr ≤ 0.83) ***Ozone:*** Approximately the same ozone profiles at upwind and summit station, downwind higher concentrations
E4	02 Oct. 2001	Excellent stable flow conditions, orographic crest cloud, incomplete data set	***LM:*** Very homogeneous flow pattern, high wind speeds (up to 10 m s^{-1}), overflow with lee waves ***Froude number:*** No deceleration (Fr $\rightarrow$ 0.0) ***Ozone:*** Approximately the same ozone profiles at all sites
E5	11 Oct. 2001	Less stable incident flow, large-scale cloudiness, relatively short cloud event	***LM:*** Complex wind field, flow around the ridge, zone of southwesterly flow over the central mountain range ***Froude number:*** Minor or no deceleration (Fr = 0.85/0.26) ***Ozone:*** Approximately the same ozone profiles at all sites
E6	26 Oct. 2001	very stable atmospheric stratification, constant synoptic conditions, blocking effects assumed, large preformed orographically induced stratus field	***LM:*** Blocking effects with flow parallel to the ridge, channelling in the Werra valley and flow around the mountain range, hydraulic jump ***Froude number:*** Stagnation (Fr = 1.58) ***Ozone:*** In the middle of the event minor differences in the ozone concentrations

References

Tilgner, A., Heinold, B., Nowak, A., Herrmann, H., 2005. Meteorological characterisation of the FEBUKO hill cap cloud experiments, Part I: Synoptic characterisation of measurement periods. Atmospheric Environment (this issue).